RoJAE

Romanian Journal of Automotive Engineering

SIAR

The Journal of the Society of Automotive Engineers of Romania
www.siar.ro
www.ro-jae.ro

RoJAE
Romanian
Journal of **A**utomotive **E**ngineering

SIAR – The Society of Automotive Engineers of Romania is the professional organization of automotive engineers, an independent legal entity, non-profit, active member of FISITA (Fédération Internationale des Sociétés d'Ingénieurs des Techniques de l'Automobile - International Federation of Automotive Engineering Societies) and EAEC (European Cooperation Automotive Engineers).

Founded in January 1990 as a professional association, non-governmental, SIAR's main objectives are: development and increase the exchange of professional information, promoting Romanian scientific research results, new technologies specific to automotive industry, international cooperation.

Shortly after its constitution, SIAR was affiliated to FISITA - International Federation of Automotive Engineers and EAEC - European Conference of Automotive Engineers, thus ensuring full involvement in specific activities undertaken globally.

In order to help promoting the science and technology in the automotive industry, SIAR is issuing 4 times a year rIA - Journal of Automotive Engineers (on paper in Romanian and electronically in Romanian and English).

The organization of national and international scientific meetings with a large participation of experts from universities and research institutes and economic environment is an important part of SIAR's. In this direction, SIAR holds an annual scientific event with a wide international participation. The SIAR annual congress is hosted successively by large universities that have ongoing programs of study in automotive engineering.

Developing relationships with the economic environment is a constant concern. The presence in Romania of OEMs and their suppliers enables continuous communication between industry and academia.

A constant priority in SIAR's activity is to ensure optimal framework for collaboration between universities and research, industry and business specialists.

RoJAE
Romanian
Journal of Automotive Engineering

CONTENTS

AERODYNAMIC PERFORMANCE EVALUATION FOR A VEHICLE STRUCTURE EQUIPPED WITH A BICYCLE RACK

Iacob-Liviu SCURTU[*]

Technical University of Cluj-Napoca, Department of Automotive Engineering and Transports, Bulevardul Muncii 103-105, 400641 CLUJ-NAPOCA, Romania

Abstract: *Nowadays, the aerodynamics of the auto vehicle's structure is conceived from the CAD design stage due to the CFD module integrated in the software environment. This research presents an aerodynamic study of a vehicle equipped with a bicycle rack. In the first part of the paper are presented some CFD aerodynamic study, theoretical aspect and the CFD software that can be used to solve the structure aerodynamics. Also, it is establishing the airflow type by calculating the Reynolds number. The three-dimensional model of the car and the bicycle rack are modelled in the second part of the paper. The model of the vehicle is designed using blueprint sketch picture that are realized on the projection plane from the drawing area from software. The vehicles body are CFD simulated using RANS equation algorithm for turbulent flow for two cases: in first case is simulated just the vehicle body and in second case is simulated the vehicle body that have attached a bicycle rack with two bicycles. Both cases are simulated at different velocity: 60, 90, 120, 150, 180, and 210 km/h. The visualization and interpreted the obtained results and conclusion of this work is presented in the last part of the paper.*

Key-Words: *CAD design, drag coefficient, aerodynamic lift, CFD simulation, airflow*

1. INTRODUCTION

Due to technological competition and the desire to reduce the fuel consumed by the vehicle, the aerodynamic body shape has been extensively studied. The first car body made according to the principles of aerodynamics was made in 1899. The Belgian Camille Jenatzy, a racing driver, managed to exceed a speed of 100 km/h with this electrically driven car [10]. In 1924, the Romanian engineer Aurel Persu presented a patented aerodynamic structure of cars under the name *"Streamline Power Vehicle"*. This vehicle has an aerodynamic coefficient of 0.22, remaining to this day in the top of vehicles with the lowest aerodynamic coefficient [6]. The use of computer and dedicated software has made it possible to quickly and correctly solve the situations imposed since the design stage of the products, having the possibility of solving iterative computational processes [1].

The software applications used include the entire area of conception, optimization, design and manufacturing of mechanical parts used in the manufacture assembly. The software versatility allows the performance of analyzes and simulations on several fields, such as the application for determining methods and maintaining the thermal comfort inside vehicles. An important aerodynamic study is performed on the Ahmed body which has an air diffuser mounted on the rear side underbody. To establish the best shape of the diffuser, three shapes are studied: a planar shape, circular shape and an elliptical shape. In order to establish the optimal shape and positioning of the air diffuser, their angle and length is systematically varied in the range of a passenger's car. After the simulation, it is found that the use of a plane diffuser has a higher efficiency for reducing the lift coefficient [2]. Another aerodynamic study of the generic car model defined by Ahmed is modelled by adding of wheels on CDF simulation to observe the airflow when using the air diffuser on the model underbody. The simulation results show that the rear wheelhouses have a major negative impact on the aerodynamics of the studied model [3]. The aerodynamics of the vehicle are influenced by the interaction of air with the elements mounted on the upper and lower side having an important role to increasing the performance of the vehicle, such as: decreasing fuel consumption, quick acceleration, decreasing of the pollutant emissions, increasing acoustic comfort inside the car, etc.

---

[*] *Corresponding author e-mail: liviu.scurtu@auto.utcluj.ro*

Loya and the authors solve a CFD aerodynamic study applied to the vehicle geometry of a CAD and compared to highlighting the differences obtained between Star CCM+ simulation software, and Ansys Workbench. The different between obtained results of the simulations are caused by the import methodology of car geometry [4]. In present study the road surface is included, appearing the "ground effect", decreasing the lift coefficient value. The main motivation of this research is to solve a preliminary evaluation of the aerodynamic influence of the bicycle rack attached to a SAV vehicle, before designing and manufacturing a rack prototype which don't have a negatively influence the aerodynamics of the car body. This car model was chosen because it is a new and trendy model nowadays. Using the ground effect makes it possible determination the results more accurately. After viewing the flow lines, a new cover design can be proposed that can be improve de aerodynamic characteristics.

2. REYNOLDS NUMBER

The air flow around the body model can have a laminar flow or a turbulent flow, this is determined by the value of the Reynolds number. Reynolds number is given by the ratio of inertial forces to viscous forces in a fluid that is subjected to relative internal motion due to the imposed velocity of the fluid. Reynolds number is a number is a dimensionless number and its expression is presented in relation 1:

$$R_e = \frac{\rho \cdot V \cdot L}{\mu} \qquad (1)$$

where,
ρ : air density, kg/m^3
V : car velocity, m/s
L: length of the vehicle, m
μ : dynamic air viscosity, kg/m·s

To determine the air flow rate around the vehicle body, the Reynolds number value is calculated for each velocity case and is shown in table 1. The value of the air density is ρ = 1,225 kg/m^3, corresponding to a temperature of 15°C, the length of the vehicle is L = 4,752 m and the dynamic air viscosity μ = 1,802 · 10^5 kg/m·s.

Table 1.
The values of the Reynolds number

Air velocity [m/s]	16.67	25	33.34	41.67	50	58.34
R_e	5.385·10^6	8.076·10^6	1.077·10^7	1.346·10^7	1.615·10^7	1.885·10^7

In the case of external flows over a flat plate is up to a value of Reynolds number Re <5x10^5 the flow is laminar. If the flow performed is between the values of 5x10^5< Re<10^7 the flow in a transient regime and at Re<10^7 the flow is turbulent. As can be seen in table 1, the resulting values of the Reynolds number indicate a turbulent airflow around the vehicle.

3. AERODYNAMICS LOAD

Aerodynamic forces value determinate in this study consist of drag force and lift force. It is known that the ration of the distribution of the aerodynamic force that acts on the car body surface are as follows: 40-45 % on the external surface, 25-30 % on wheels housing and 20-25 % from the underbody of the body and engine area [7]. Figure 1a shows forces that act on the vehicle when driving on the road. The expression of the traction force is presented in relation 2.

$$F_T = F_D + F_R + m\frac{dV}{dt} + m \cdot g \cdot \sin\alpha \qquad (2)$$

F_D : drag force, N
F_R : friction force at rolling, N
m : mass of the vehicle, kg
α : angle of road inclination, °
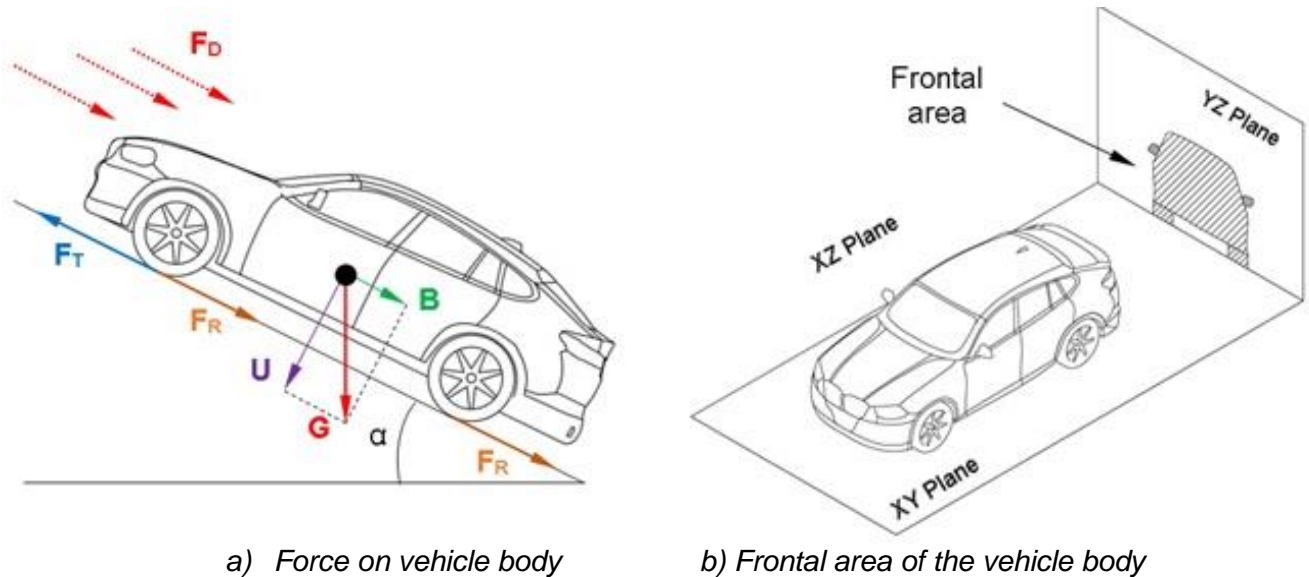
a) Force on vehicle body   *b) Frontal area of the vehicle body*
Figure 1. Force that acts on the vehicle body and frontal area view [7][8]

The value of the drag force depends by the mass of the vehicle and friction coefficient on wheels rolling. Expression 3 presents the equation of the rolling resistance force.

$$F_R = f_R \cdot G \tag{3}$$

where,
f_R : friction coefficient on wheels rolling
G : gravitational force (G=m*g)

3.1 Drag force

The main force that acts on the vehicle body during driving is the drag force, which is given by the characteristic of the fluid to resist the advance of a car. In automotive aerodynamics, the axis on which drag force acts is conventionally chosen on the X axis. The size of this force is influenced by the running speed of the vehicle, the density and mechanical properties of the air and the exterior geometry of the car. The expression of the aerodynamic force is given by relation 4. Relation 5 present the expression of the drag coefficient deducted from the expression of the drag force.

$$F_D = \frac{1}{2} \rho \cdot C_D \cdot A \cdot V^2 \tag{4}$$

C_D : drag coefficient
A : cross-sectional area of the vehicle body, m^2
V : car velocity, m/s
ρ : air density, kg/m^3

$$C_D = \frac{2 \cdot F_D}{\rho \cdot A \cdot V^2} \tag{5}$$

3.2 Lift force

In vehicle aerodynamics the lift force can be defined as the sum of all forces generated around the car body which is projected on a perpendicular plane to the air flow direction during travel. The term used to name this force is "lift", used especially in aeronautics that makes it possible to hold the plane in the air. This mechanical force results from the interaction between a solid body and a fluid, in this case between the car and the air. The lift force can also have a negative value; this being oriented towards the road. If the load value has a high negative value on the car's tires, an additional pressure is exerted, which implies a premature tire wear and implicitly an increase fuel consumption,

if the load force is too high there may be a risk of losing control of the car, due to its too small adherence. For the lift force, the Z axis is conventionally chosen as the driving direction.
The expression of the lift force is presented in relation 6.

$$F_L = \frac{1}{2}\rho \cdot C_L \cdot A_L \cdot V^2 \tag{6}$$

$$C_L = \frac{2 \cdot F_L}{\rho \cdot A_L \cdot V^2} \tag{7}$$

C_L – lift coefficient
A_L - area of the vehicle body on the ground [m^2]
The value of the lift coefficient is given by the relation 7, presented above.

4. CAD MODELLING

Car geometry modeling was done by SolidWorks software using advanced modeling techniques applied for surface generation [11]. The three-dimensional model of cars is made with the help of "blueprint" pictures introduced in the working area of the software [9]. The geometry of the car is modeled approximately by the shape and overall dimensions of the BMW X4. Figure 2a shows an intermediate stage in the body modeling process using the surface drawing module. The CAD model was generated in two modeling stages: in the first stage the body geometry of the car was modeling for the first simulation case, and in the second stage the bicycle rack is attached to the car body.

a) Surface modelling   b) Final model of the vehicle body whit bicycle rack
Figure 2. CAD modelling

Figure 3. Overall dimensions of the final model
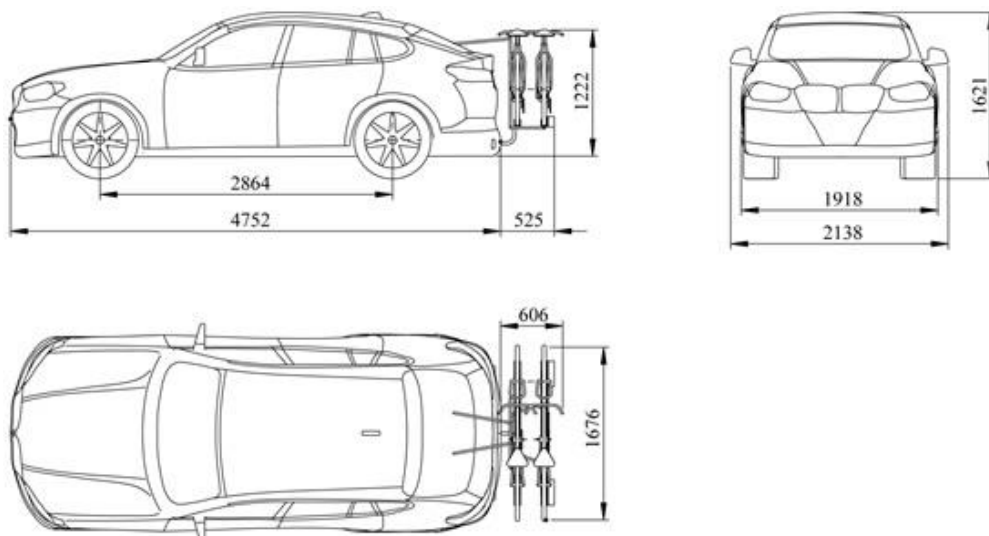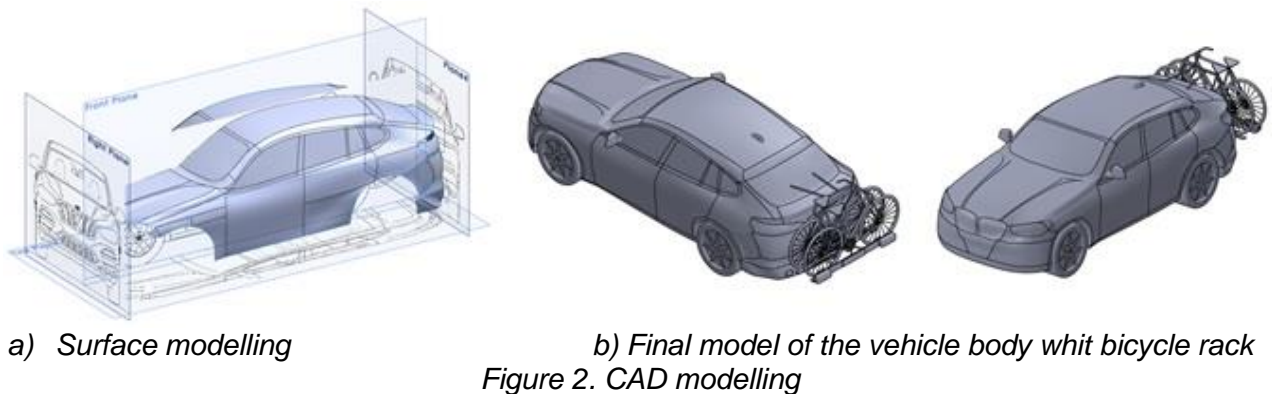
To view the shape of the car body, the position of the bicycle rack and the overall dimensions in figure 3 is presented the triple projection of the final model. The cross-sectional area of the vehicle body value used for determining the drag coefficient is 2.67 m^2 and the area of the vehicle projected on the road surface is m^2. All surface area is measured in CAD software environment.

5. CFD APROACH

Performing a CFD simulation involves completing the steps presented in figure 4. The start point of the CFD simulation process is given by the CAD modeling of the car body and includes the model in the CFD simulation environment. The step of defining the computational domain is very important because depending on the dimensions of this computational domain, the results can be viewed correctly.

Figure 4. CFD process

The discretization step of the calculation domain can be performed automatically or manually, choosing an optimal size of the meshed elements. Discretization can be achieved gradually by imposing a smaller size in the important areas to be studied on the surface of the CAD model. Applying the imposed boundary simulation conditions presents the next step for performing the CFD simulation process.

The start of the solver presents the stage in which the user has the minimum input, the whole calculation process being performed by the software. In the last stage of the CFD process the obtained results are visualized and interpreted.

The CFD simulations from this study is determined by the Reynolds-Averaged Navier-Stokes (RANS) equations for the incompressible turbulent flow and the k-ω turbulence model with the Shear Stress Transport (SST) [5].

The expression of the continuity equation of the used RANS is presented in relation 8:

$$\frac{\partial \overline{v}_j}{\partial x_j} = 0 \tag{8}$$

In the next relation is presented the expression of the momentum equation:

$$\frac{\partial}{\partial x_j}\left(\overline{v}_j\overline{v}_j\right) = -\frac{\partial \overline{p}}{\partial x_i} + \frac{\partial \overline{p}}{\partial x_j}\left[\mu\left(\frac{\partial \overline{v}_i}{\partial x_j} + \frac{\partial \overline{v}_j}{\partial x_i}\right) + \mu_t\left(\frac{\partial \overline{v}_i}{\partial x_j} + \frac{\partial \overline{v}_j}{\partial x_i}\right) - \frac{2}{3}\rho\overline{k}\delta_{ij}\right] \tag{9}$$

Where,
$\overline{v}_i$: mean of the airflow velocity
x_i : coordinates
$\overline{p}$: averaged air pressure
μ_t : turbulent viscosity
$\overline{k}$: averaged turbulence kinetic energy
The averaged turbulence kinetic energy equation is presented in expression 10:

$$\overline{k} = \frac{\overline{v_i'v_i'}}{2} \tag{10}$$

This iterative process started using the first order numerical scheme and the second order close the numerical scheme.

9

5.1 Computational domain and boundary conditions

The virtual simulation domain is designed in order to imitate the real environment while driving on the road. In this paper the drag force and the drag coefficient are calculated for the geometry of the vehicle that is placed on the road surface. Adding the road in the simulations appears the phenomenon called in aerodynamics "ground effect". In this case, this effect is the result of the interaction between the air and the geometry of the vehicle when it moves on the road surface. The virtual wind tunnel is represented by the calculation volume in which it will be possible to see the behavior of the air flow around the car body. The computational domain for the study is presented in figure 5. For a detailed analysis of the air flow, the geometry of the vehicle is placed at a distance of 1.5 m from the air intake, the length of the tunnel is 30 m and the height are 4 m.
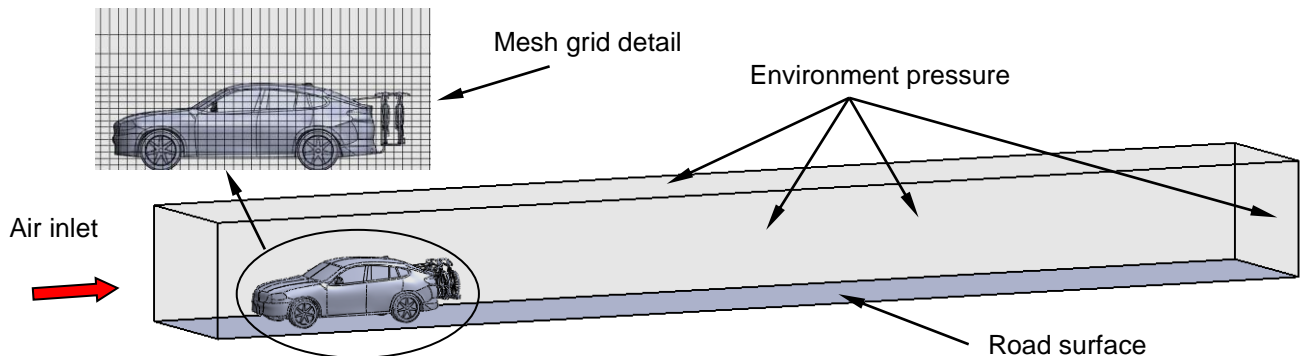
Figure 5. Boundary conditions in computational domain

For a higher accuracy of the CFD simulation, the discretized layers near the surfaces are denser, respectively the number of elements is higher, compared to the other elements, like can be seen in mesh grid detail from figure 5. The computational domain is discretized for the first simulation case in 110352 cells, of which 12097 cells are in contact to the vehicle surface and the second simulation model that contain the bicycles rack is discretized in 116485 cells, of which 13951 cells are in contact with the three-dimensional model surface of the vehicle and the bicycles rack.

The CFD simulation was performed for two cases: the first case in which the vehicle is running on the road and the case in which a support with two bicycles is mounted in the back. Both simulation cases are performed at different velocity: 60, 90, 120, 150, 180, 210 km/h. In the simulation have being taken into account the effect of the road.

5.2 Simulation result of the car base model

In this section are presented the visual and the numerical result obtained for both simulation cases: the simulation of the car body and the simulation of the car body that have attached the bicycle rack whit two bicycles.
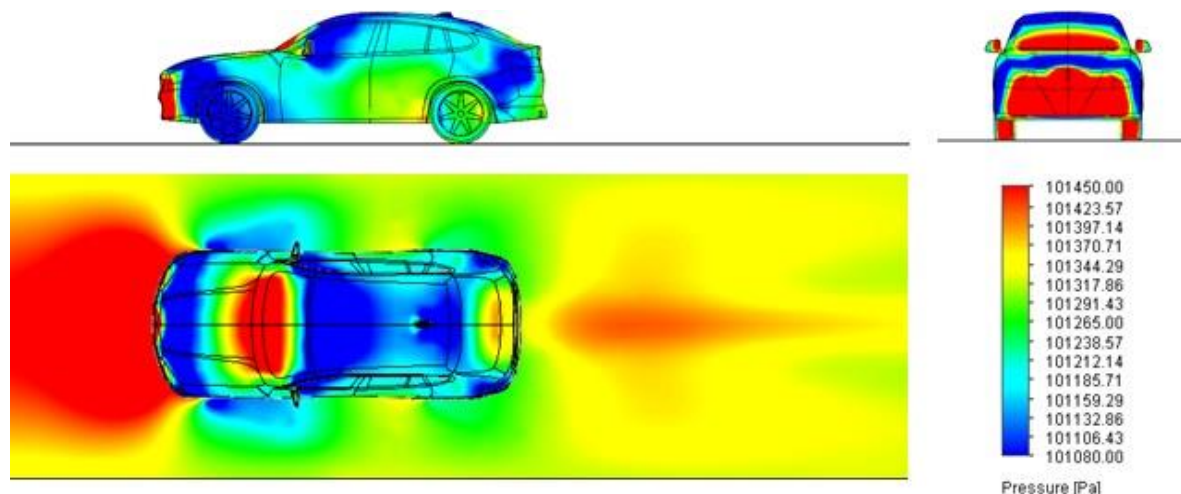
Figure 6. Pressure distribution at 33,34 m/s velocity

In figure 6 is presented the pressure distribution on the body car surface and the read surface.
It can be observed than in the front of the car on the road surface the pressure value has a maxim value. On the vehicle surface the maximal value of the air pressure is situated on the front side of the car body, on the bumper, front wheels, lower side of the windshield and the front mirror surface. The pressure distributions it presented at 33.34 m/s velocity of the wind. In the rear side of the vehicle the air pressure is lower which show that car geometry is manufactured after aerodynamic study. For a better view of the pressure distributions in figure 7 is presented two pictures that show the axonometric view of the car model. The range presentation in the pictures is 101080 - 101450 Pa.
Figure 8 shows the velocity streamline distribution on the car body surface and the road surface. It can be observed that in the area of the wheel housing and the rear side vortices are generated. For a better view of airflow on the car body the pictures are cropped just in the body car zone. Isometric representation of the streamline velocity is presented in figure 9, where can be observed the effects of the airflow around the car body.
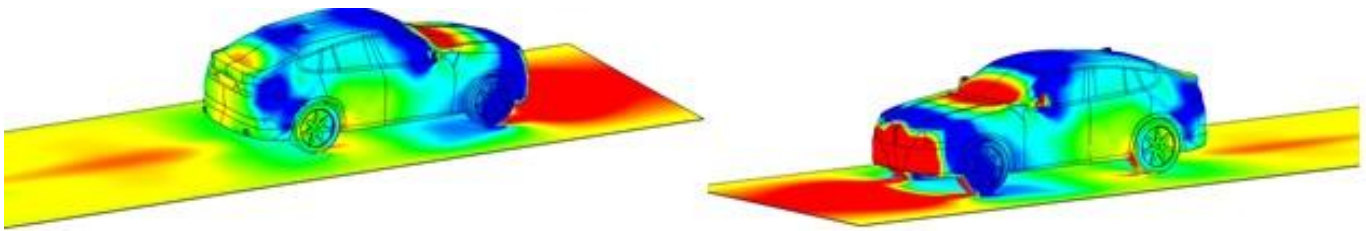
Figure 7. Axonometric view of the pressure distribution at 33,34 m/s velocity
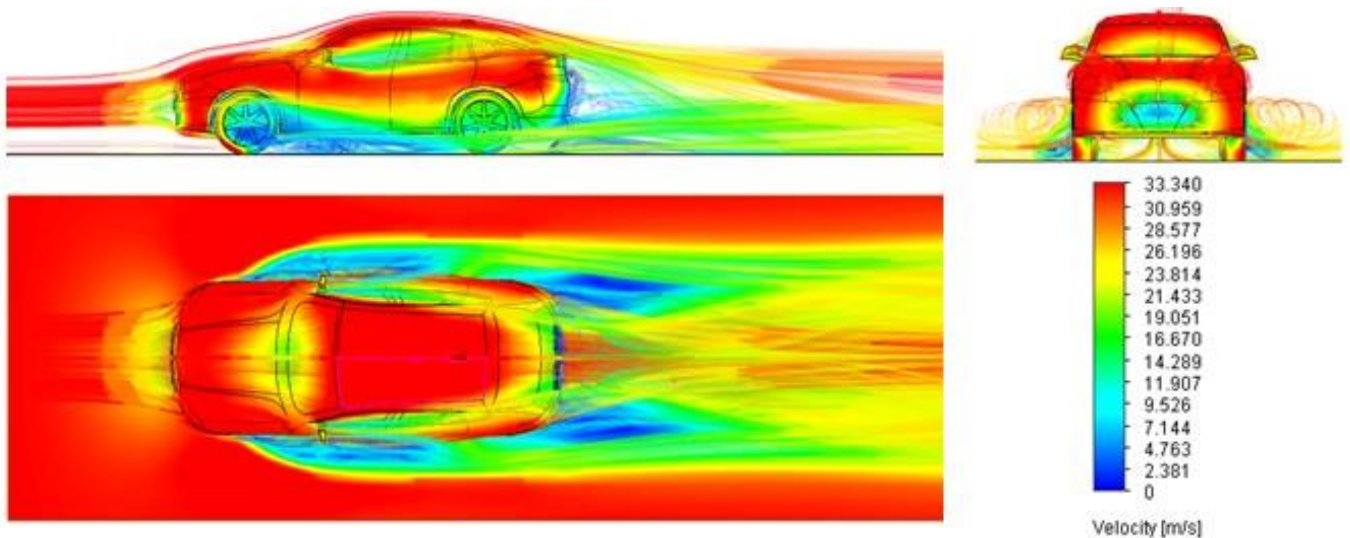
Figure 8. Airflow at 33,34 m/s velocity
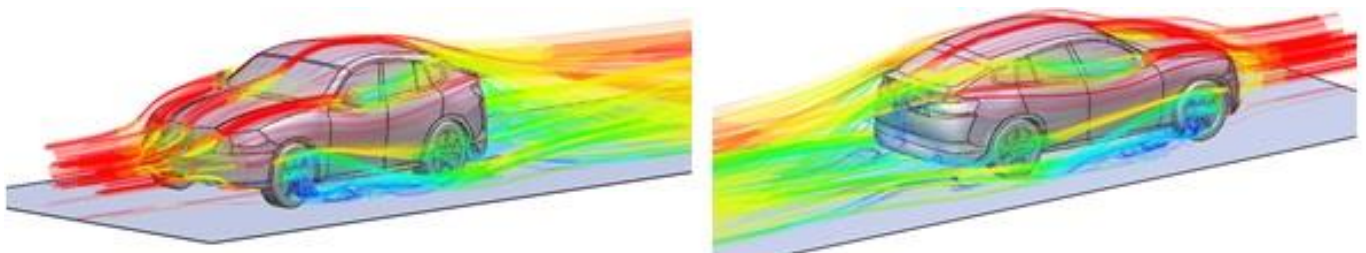
Figure 9. Isometric view of the airflow at 33,34 m/s velocity

The numerical results of the first simulation case are presented in table 2, where are presented the resulted value of the drag force, lift force and computed value of the drag and lift coefficient.

It can be observed that the drag force increases according to the air velocity, the range of the drag force values is 202.386 – 2397.84.
The value of the drag coefficient remains constant during all simulations.

Table 2.
Numerical results of the car base model

Air velocity [km/h]	Air velocity [m/s]	Drag force [N]	Drag coefficient	Lift force [N]	Lift coefficient
60	16.67	197.862	0.435	12.255	0.008
90	25	442.605	0.433	30.784	0.008
120	33.34	781.766	0.432	52.149	0.008
150	41.67	1209.880	0.426	74.094	0.007
180	50	1736.830	0.424	108.271	0.007
210	58.34	2348.730	0.422	141.740	0.007

5.3 Simulation result of the car model whit bicycle rack

Adding the bicycle rack in the simulation modifies the pressure distribution on the vehicle surface. It can be observed that the pressure distribution on the front side of the vehicle still unchanged compared to the first simulation results. In the rear side of the car the pressure distribution is higher on the hatchback as can be seen in figure 10. The lower values of the pressure are distributed on the behind door surface and the roof surface. In figure 11 can be viewed the pressure distribution on the vehicle surface and the bicycle rack. The pressure distribution on the road surface is a little bit smaller than in the simulation case without bicycle rack.
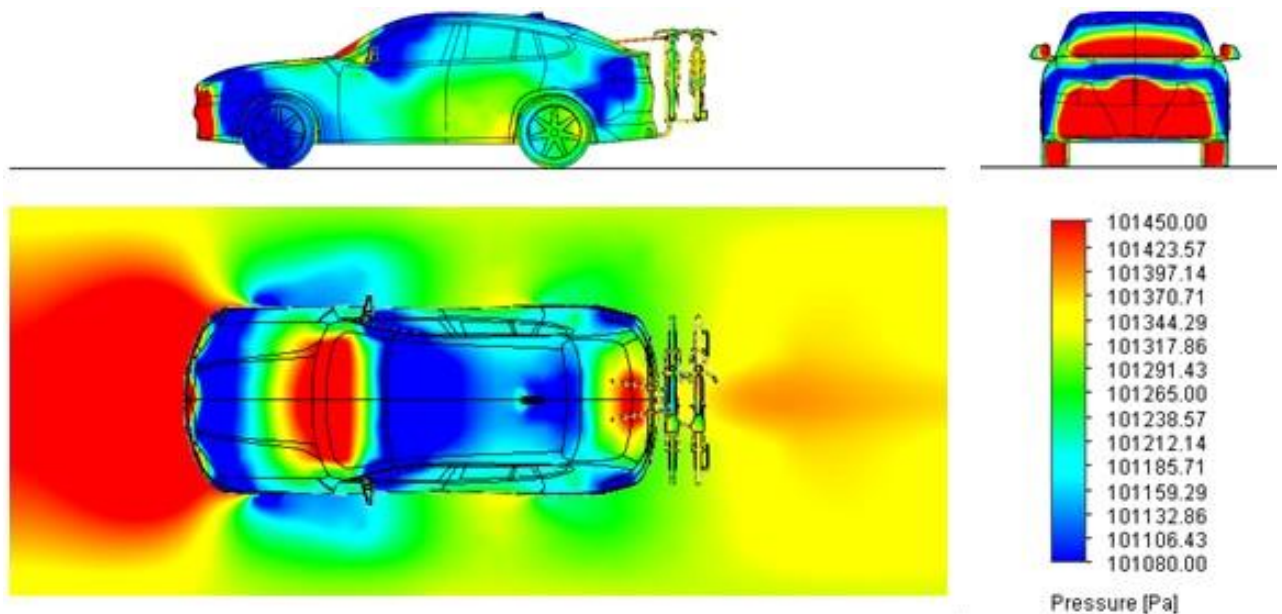
Figure 10. Pressure distribution at 33,34 m/s velocity of the model with bicycle rack
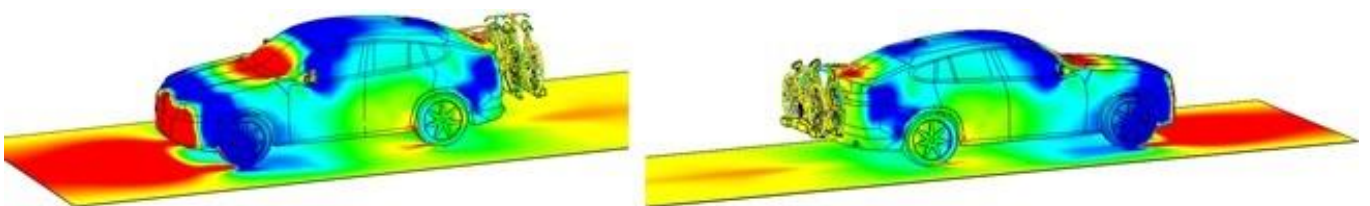
Figure 11. Isometric view of the pressure distribution at 33,34 m/s velocity of the second model
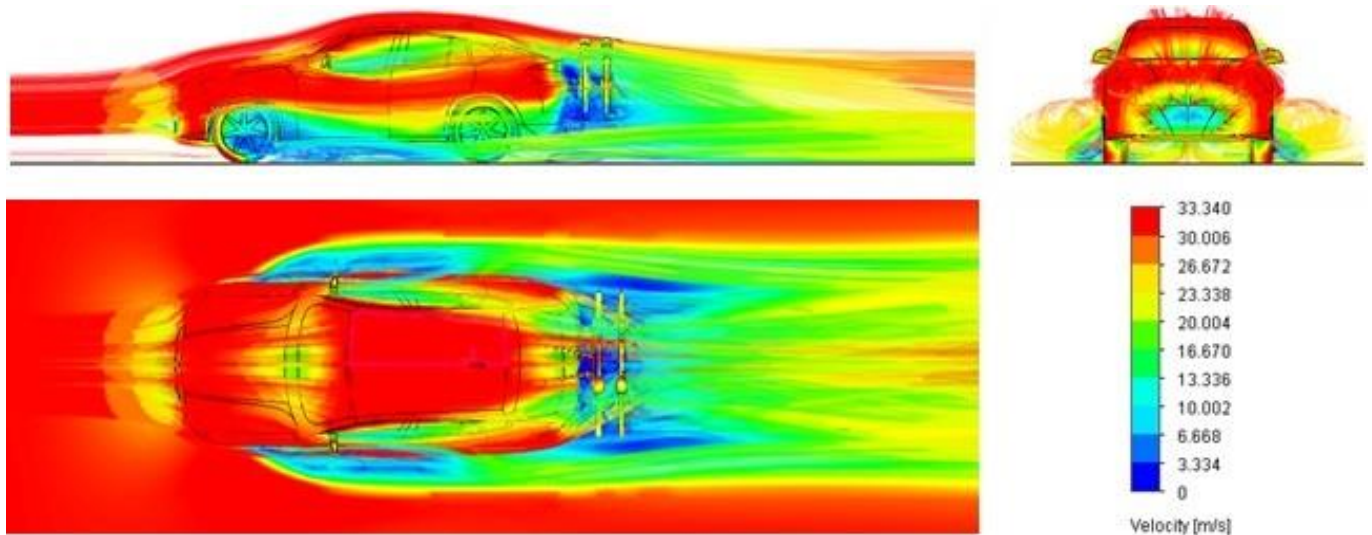
Figure 12. Airflow at 33,34 m/s velocity of the model with bicycle rack

The airflow dynamics is observed in figure 12 for the model that contatin the bicycle support, where in the rear side of the vehicle in bicycle rack area the air velocity decreas suddenly resulting a vortex that has an negativ impact in the vehicle aerodynamics.
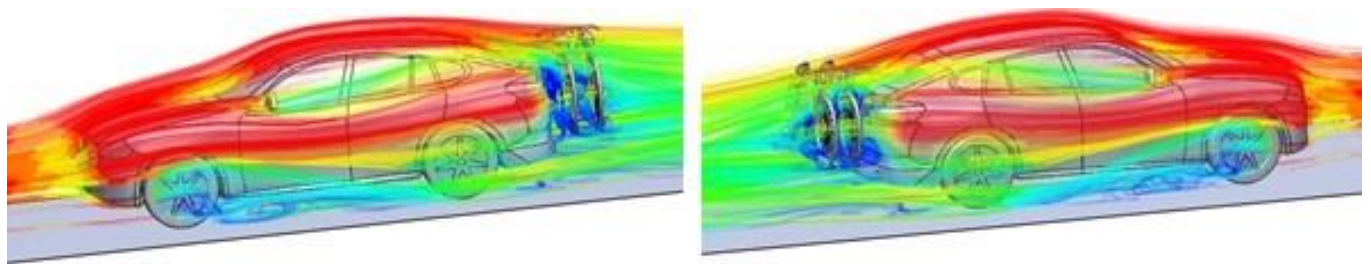
Figure 13. Isometric view of the airflow at 33,34 m/s velocity of the second model

A better view of the streamline airflow for this vehicle model is presented in figure 13, where can be viwed the airflow turbulence. In table 3 are written the resulted values of the CFD second studies.
Analyzing the result obtained in table 2 and 3 it can be observed that the drag force values increase relative to the airflow velocity.
The value of the drag and lift coefficient remains approximately constant.
The lower values of the lift coefficient are due to the road surface effect.

Table 3.
Numerical results of the second simulation case

Air velocity [km/h]	Air velocity [m/s]	Drag force [N]	Drag coefficient	Lift force [N]	Lift coefficient
60	16.67	202.386	0.445	12.761	0.008
90	25	452.015	0.442	29.193	0.008
120	33.34	797.15	0.438	46.574	0.007
150	41.67	1235	0.434	68.397	0.007
180	50	1769.98	0.432	92.497	0.006
210	58.34	2397.84	0.430	130.948	0.007

6. CONCLUSION

This aerodynamic study was performed by adding the "ground effect" presented by the car's roadway. For establishing the aerodynamic performance, the CAD models are CFD simulated for six velocity cases. Comparing the obtained result in both cases it can be observed that the values resulted at the vehicle with the bicycle rack have higher values than the vehicle without bicycle rack. In both simulation cases the values of the drag and lift coefficient remains approximately constant for all velocity simulation cases. The average value of the drag coefficient of the vehicle simulated in first case is 0.429 and for the vehicle with bicycle rack is 0.437. The difference between the values obtained in both cases is relatively small and does not influence much negatively the aerodynamics performances of the vehicles. The visual representation of the result from this paper was made at a 120 km/h velocity because this is a reference velocity for establishing the drag coefficient.

REFERENCES

[1] Balcau M, Cristea AF. *Theoretical considerations regarding the dynamic absorber,* Acta Technica Napocensis-Series: Applied mathematics, mechanics, and engineering. 62(3), 2019

[2] Huminic, A., Huminic, G. *Aerodynamic study of a generic car model with wheels and underbody diffuser,* Int.J Automot. Technol. 18, 397–404, https://doi.org/10.1007/s12239-017-0040-6, (2017)

[3] Huminic, A. and Huminic, G., *Aerodynamics of curved underbody diffusers using CFD,* Journal of Wind Engineering and Industrial Aerodynamics, 205, p.104300,
https://doi.org/10.1016/j.jweia.2020.104300, 2020

[4] Loya, A., Iqbal, A., Nasir, M.T., Ali, H., Khan, M.Z.U. and Imran, M., 2019. *Automotive Aerodynamics Analysis Using Two Commonly Used Commercial Software.* Engineering, 11(01), p.22.

[5] Majdandžić, L., Buljić, D., Buljac, A., & Kozmar, H. *Aerodynamic design of a solar road vehicle.* International Journal of Automotive Technology, 19(6), 949-957, 2018.

[6] Persu, A., *Streamline Power Vehicle.* In: United States Patent Office, Serial no: 671,727, 1923.

[7] Sebben, S., Walker, T. and Landström, C., 2014. *Fundamentals, Basic Principles in Road Vehicle Aerodynamics and Design.* Encyclopedia of Automotive Engineering, pp.1-16.

[8] Todoruţ, A., Cordoș, N., Burdea, M.D., Bălcău, Monica, *The evaluation of normal load redistribution on the static axles and on the wheels, when the vehicle is in motion*, Cluj-Napoca, Acta Technica Napocensis, Series: Applied Mathematics, Mechanics, and Engineering, Vol. 58(3), pg. 349-360, Ed. U.T.PRESS, ISSN 1221-5872, 2015

[9] https://drawingdatabase.com/bmw-x4-2018/ , accessed 2020

[10] https://academiaromana.ro/sectii/sectia08_tehnica/doc2020/IstoriaTehnicii/25Istoria Tehnicii-Vol2.pdf

[11] Solidworks help tutorials 2018

STUDY OF THE INFLUENCE OF ROOF LUGGAGE BOX ON A VEHICLE AERODYNAMICS

Ancuta-Nadia JURCO[*]

Technical University of Cluj-Napoca, Department of Automotive Engineering and Transports,
Bulevardul Muncii 103-105, 400641 CLUJ - NAPOCA, Romania

Abstract: *This research presents an aerodynamic comparative study between a base car body and a car body equipped with a roof luggage box. The car model and the luggage box are designed according to the overall dimensions of the commercial model. In the first part of the paper is presented some recent aerodynamic study using iterative calculation methods, followed by the presentation of the theoretical aspects, also the airflow regime is established by calculating the Reynolds number. In the second part of the paper the CAD modelling of the car and the CFD boundary conditions and mesh grid are generated. The simulation methodology is performed by using the RANS time averaged equations supplemented by (k- ε) turbulence model. In the third part of the paper the CFD simulations are solved for five airflow velocity for each case. The results of the study are compared, and it can be observed that the car equipped with luggage box results a higher aerodynamic coefficient. The conclusion of this study is presented in the last part of this the paper.*

Key-Words: *Aerodynamic drag, CFD, CAD, Computational domain.*

1. INTRODUCTION

Nowadays the computer is an integral tool in the designing process of product manufacturing. Actual software packages contain modules that can solve problems related to vibrations and stability of shock absorbers that are part of the vehicles structure [1], calculations to establish the thermal comfort inside vehicles and crash simulations of structural components of vehicles [9]. Software which contain iterative CFD calculation methods can be used solve external fluid simulation problems in order to establish geometric parameters for the design of the car bodies or auxiliary automotive parts such as side mirrors [8], [10]. The aerodynamic drag is influenced by the geometry of the side mirrors, the geometry of the underbody and the ground clearance. The mirrors of the new car models are replaced by the video cameras, so the dimension of the support is reduced. The underbody geometry is covered by protective shields and air deflectors that can guide the airflow to reduce the turbulence. The ground clearance of the car body can be automatically reduced after the car exceeds a high speed, increasing the stability on the road and lowering the aerodynamic coefficient. An aerodynamic study that establishes the car aerodynamics caused by the underbody geometry of the car is carried out, finding that the flat geometry of the air diffuser has an important role in achieving a forward effect and a higher down force. [4]. The car body shape and the auxiliary equipment influences the aerodynamic coefficient, determining an increase in fuel consumption. For this reason, the aerodynamic study is necessary to determine the best aerodynamic shape that has an aerodynamic lower drag coefficient. Auxiliary equipment occasionally mounted on the car is the roof luggage box. The shape of this equipment increases the fuel consumption. An aerodynamic shape of a roof luggage box is studied and optimized by reducing drag force by 34% resulting to a 1.7% fuel saving compared to the base model [6]. Another aerodynamic study is one in which it is examined the influence of the position of the roof luggage box for the DriverAer body and uses the RANS turbulent simulation model using the commercial software Ansys Fluent [5].

This study is focused on assessing the aerodynamic influence of the car equipped with a roof luggage box. Performing the aerodynamic simulation of the roof luggage box together with the car provides a more and complete detail of the aerodynamics influence behind the car body. After conducting this study, a luggage box design can be proposed to be particularly adapted to this type of car.

---

[*] *Corresponding author e-mail:* ancuta.jurco@auto.utcluj.ro

2. MATHEMATICAL APROACH

2.1 Reynolds number

In aerodynamics studies the value of the Reynolds number establishes the airflow regime around the car body. Fluid flow can occur in two modes of movement, different in terms of their structure: laminar flow and turbulent flow [3]. Reynolds number is calculated according to the formula presented in relation 1, at air density $\rho = 1.205$ kg/m^3, length of the vehicle L=4.484 m, dynamic air viscosity $\mu = 1.825 \times 10^{-5}$.

$$R_e = \frac{\rho v L}{\mu} \tag{1}$$

Table 1.
Reynolds number values for reference velocity

Velocity [m/s]	11.11	22.22	33.33	44.44	55.56
R_e	3.289×10^6	6.579×10^6	9.868×10^6	1.316×10^7	1.645×10^7

If the Reynolds number has a high value, the airflow is turbulent.
To determine the flow rate in this study, the value of the Reynolds number presented in table 1 was calculated, finding that the flow rate is turbulent for each airflow velocity around the car.

2.2 Mathematical model

Mathematical modelling of the airflow simulation process around the vehicle model is performed using the Reynolds Averaged Navier Stokes (RANS) system of equations [7]. Navier-Stokes equations are nonlinear partial differential equations. Due to the nonlinearity, solve of these equations can be impossible, especially in the case of turbulent flows. For CFD calculations, the RANS time averaged equation is used and supplemented a turbulence model (k- ε).
In the Cartesian tensor form these equations can be written:

$$\frac{\partial U_i}{\partial x_i} = 0 \tag{2}$$

$$\rho = \frac{\partial}{\partial x_j}\left(U_j U_i + \overline{u_j' u_i'} \right) = -\frac{\partial P}{\partial x_i} + \frac{\partial}{\partial x_j}\left(2\mu S_{ij} \right) \tag{3}$$

Where,
U_i : mean of velocity tensor
x_i : vector position
$\overline{u_j' u_i'}$: average of fluctuating velocity
P : mean static pressure
μ : molecular viscosity

The strain rate expression is given in next relation:

$$S_{ij} = \frac{1}{2}\left(\frac{\partial u_i}{\partial x_j} + \frac{\partial u_j}{\partial x_i} \right) \tag{4}$$

The standard k-ε turbulence model is given in next equation:

$$\rho U_j \frac{\partial k}{\partial x_j} = \tau_{ij} \frac{\partial U_i}{\partial x_i} - \rho \varepsilon + \frac{\partial}{\partial x_j}\left[\left(\mu + \frac{\mu_T}{\sigma_k} \right) \frac{\partial \varepsilon}{\partial x_j} \right] \tag{5}$$

where,

τ_{ij} : Reynolds stress
μ_T : turbulent viscosity
σ_k : closure coefficient
ε : dissipation rate

Dissipation rate of turbulence kinetic energy equation is given in the next relation:

$$\rho U_j \frac{\partial \varepsilon}{\partial x_j} = C_{\varepsilon 1} \frac{\varepsilon}{k} \tau_{ij} \frac{\partial U_i}{\partial x_j} - C_{\varepsilon 1} \rho + \frac{\varepsilon^2}{k} + \frac{\partial}{\partial x_j}\left[\left(\mu + \frac{\mu_T}{\sigma_\varepsilon}\right)\frac{\partial \varepsilon}{\partial x_j}\right]$$

(6)

The expression of the turbulent viscosity is:

$$\mu_T = \rho C_\mu \frac{k^2}{\varepsilon}$$

(7)

For closure of the RANS equations, it is used the turbulence model Shear-Stress-Transport (SST).

2.3 Aerodynamic load on the vehicle body

During the vehicles driving, on the body surface acts the aerodynamic force which opposes the movement. When the air hit the surface geometry of the vehicle, on the car appears a lift force due to the passage of air under the car body. If the lift force has a high value, it can destabilize the vehicle on the road, this negative effect can appear while driving a car and it is caused by the high value of air pressure which affect the car's tires. The swirl resulted at the rear of the car appear due to the geometry of the body and the auxiliary elements with which it is equipped. In relation 8 is presented the expression of the aerodynamic force, which is exerted by the wind on the car body [2]. The distribution of the moments, forces and reaction forces that occur during the operation of the car on the road are presented detailed by Todorut and authors in a study that evaluates the load distribution on the axles and wheels of the car when it is on the road [12].
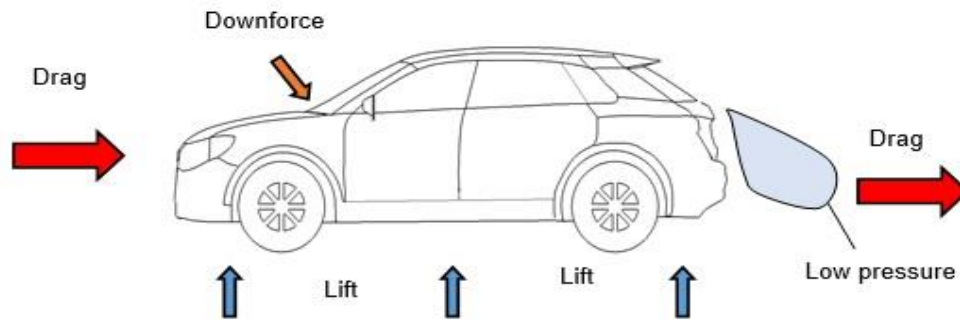
Figure 1. Aerodynamic force on the car body

$$F_x = \frac{1}{2} \cdot \rho \cdot V^2 \cdot C_D \cdot A$$

(8)

The aerodynamics of a vehicle is given by the value of the aerodynamic coefficient, which is calculated with the expression 9.

$$C_D = \frac{2 \times F_x}{\rho \times V^2 \times A}$$

(9)

where, ρ is the air density, V is the air velocity, A is the frontal area of the body car and C_D is aerodynamic coefficient.

3. CFD ANALAYSIS

Most CAD-assisted design software's have also integrated finite element simulation, fluid simulation and shape optimization modules. A widely used software for its versatility is SolidWorks, developed by Dassault Systems [14]. Using this software, it can be performed all the necessary steps to solve the aerodynamic simulation presented in this study. For obtaining and visualizing the results the CFD process include three several stages. All stages of the process are represented by preprocessing, processing and postprocessing. in figure 2 it shows the diagram of the CFD simulation stage [10].
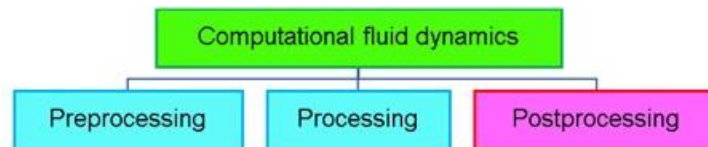

Figure 2. The stages of the CFD process

In the preprocessing step, the CAD geometry of the model is included in the fluid simulation environment, after which the loading case is performed, and the computational domain is defined. The fluid volume is meshed into finite elements, choosing an optimal discretization size. Also, in this stage the boundary conditions are imposed. In the processing stage, the model is running for different cases. The calculation time of the process depends on the accuracy result imposed in the preprocessing stage, by the size of the CAD model and on the technical characteristics of the calculation equipment.
Post-processing is the last stage, in which the obtained results can be visualized and interpreted.

3.1 Cad design
The CAD model of the generic car body is modeled from the blueprints photo of an Audi Q3 car model [13]. The sketches of the body are positioned on the projection planes in the working area of the modeling software. The exterior surfaces of the body are generated step by step by drawing sketches. Because the body model is symmetrical to the longitudinal axis, the surfaces of the car body are modeled just for half of the model and this is mirrored from the middle plane, as can be seen in figure 3a. The final model of the car resulting from the modeling process is presented in figure 3b. Figure 4 present the overall dimensions of the vehicle and the roof luggage boxes resulted after the modeling process.
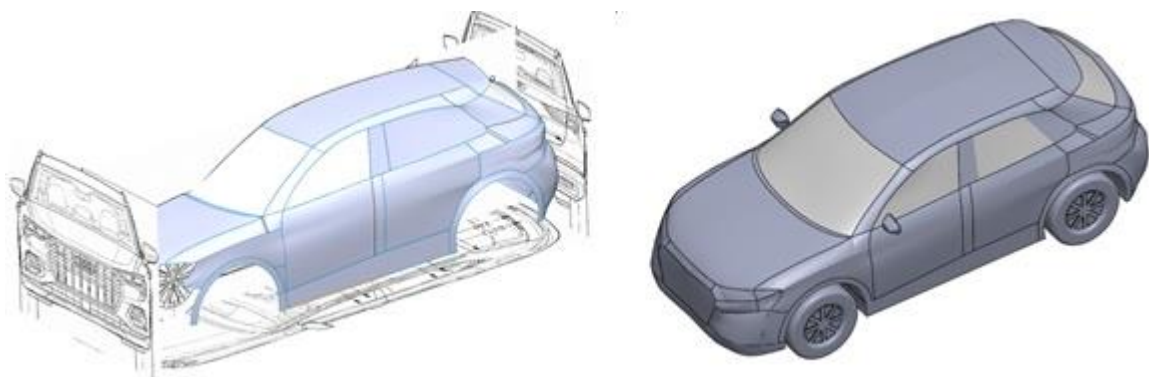
a) *External surface modelling*   b) *CAD model*
Figure 3. Car body modelling

3.2 Boundary conditions and mesh grid generation

Positions of the car body in the CFD computational domain it chosen to observe the behavior of the air flow when hit the car body and the turbulent flow that remain in rear side of the car. Figure 5 shows the location of the vehicle in the calculation range. The front side of the body is positioned to a distance at 2 m from the limit of the air inlet, respectively from the place where the air flow begins. The computational domain width is 4 m, the 4 m high and 25 m long. The direction of air flow is oriented in the opposite direction of the car running.

After establishing the computational domain, it is discretized into 26,436 fluid cells, of which 1602 cells come in contact with the body surface. In this study determination of the drag coefficient and the drag force is made without applying the ground effect of the road. In figure 6 is presented the mesh grid of the element's distribution in computational domain. For a greater accuracy of the calculations and also for the reduction of the simulation time it was chosen around the car body surface the layer elements are denser and depending by the distance from the car surface the elements size increases gradually. The determination of the value of the drag coefficient is performed by applying expression for computing drag coefficient, and the air density is 1,205 kg/m^3, value chosen for the simulation at an air temperature of 20°C. The measured area of the frontal surface of the body is 2.6 m^2, and of the luggage box is 0.15 m^2.
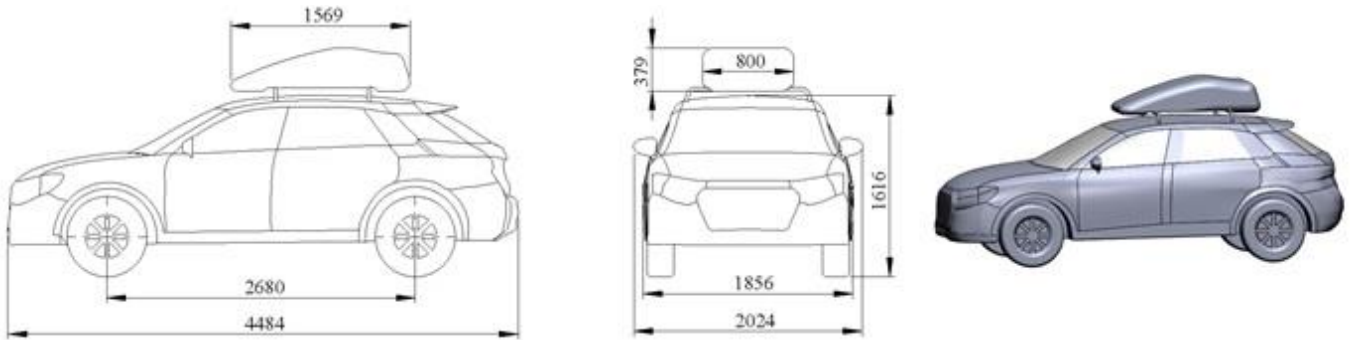
Figure 4. The overall dimensions of the body car and of the roof luggage boxes.
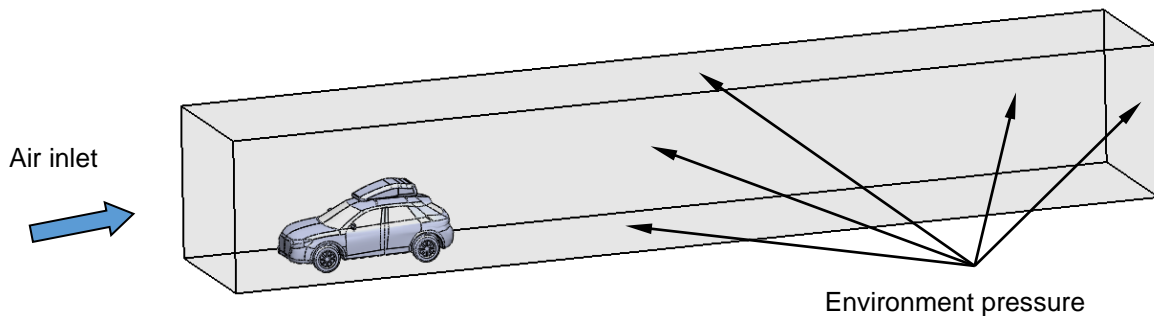
Figure 5. The car body into computational domain
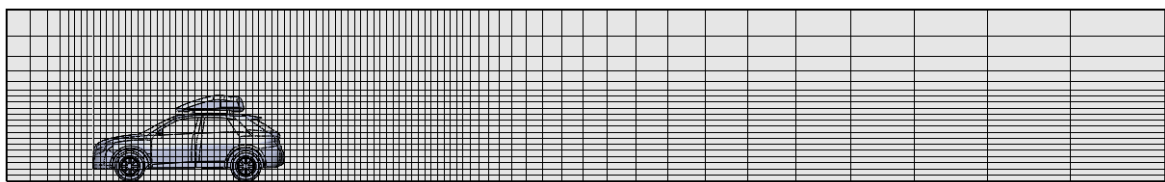
Figure 6. Mesh grid generation

4. RESULTS

The obtained results are presented for each simulation case, in table 2. To reduce the space occupied by the pictures, the presentation of the visual results was chosen only for the case when the air velocity is 33.33 m/s, for the other cases the numerical results are writing in the table.

4.1 Simulation result for base model

4.1.1 Velocity
The distribution of the airline's velocity is presented in the range of 0 - 33.33 m/s in figure 7 in orthogonal projections. It can be seen that the air velocity decreases considerably in the front of the body, in the area of the wheel housings, in the area of the exterior mirrors and in the rear side of the car, where a vortex is created.
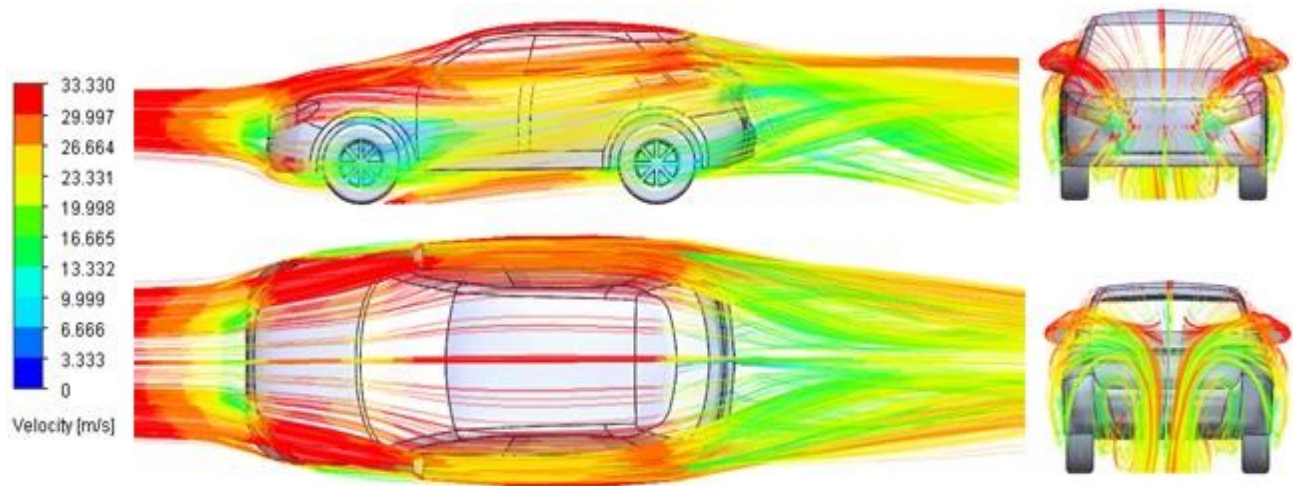
Figure 7. Air flow visualization at 33.33 m/s velocity

4.1.2 Pressure

The maximum values of the air pressure exerted on the frontal area of the body, has on the bumper surface, hood, and windshield. The minimum values of the pressure are located on the surface of the ceiling and of the ceiling support pillars, as can be seen in in figure 8.
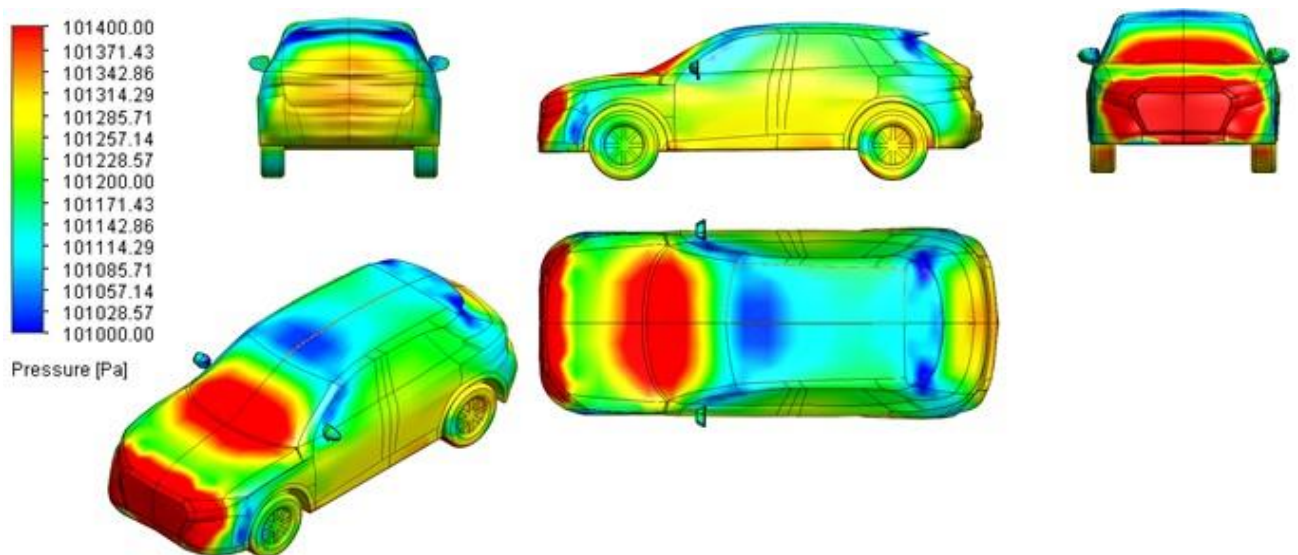
Figure 8. Visualization of the pressure exerted by the air force on the vehicle surface

4.2 Simulation result for model whit luggage carrier

4.2.1 Velocity

When the luggage compartment is placed on the upper side of the body, the airflow is no longer fine, generating turbulence in the rear side of the luggage compartment, as can be seen in figure 9.
The representation of the visual results at a speed of 33.33 m/s have been chosen because of the air distribution on the vehicle surface almost same, being different only the actuation intensity.

4.2.2 Pressure distribution

The surfaces of the car body on which the air pressure have maximum values are the surface of the front part of the body and on front part of the trunk. It can be seen in figure 10 that the minimum pressure is on the surface of the side windows behind the side mirrors and on the rear pillars in the upper area of the rear window. Due to the geometry of the luggage carrier in the rear side of the vehicle body the airflow is affected creating a small turbulence.

An important aspect is the frontal shape of the luggage carrier which is flattened to break the air.
Table 2 shows the obtained results after simulating the two cases at five different air speeds. It be seen that the value of the drag force increases with increasing the air velocity, and the value of the drag coefficient remains constant. Compared between these two cases there is an increase of the drag force and of the drag coefficient in the case of simulating the body model with luggage compartment.
The luggage compartment imposed an increasing drag force depending by the air velocity.
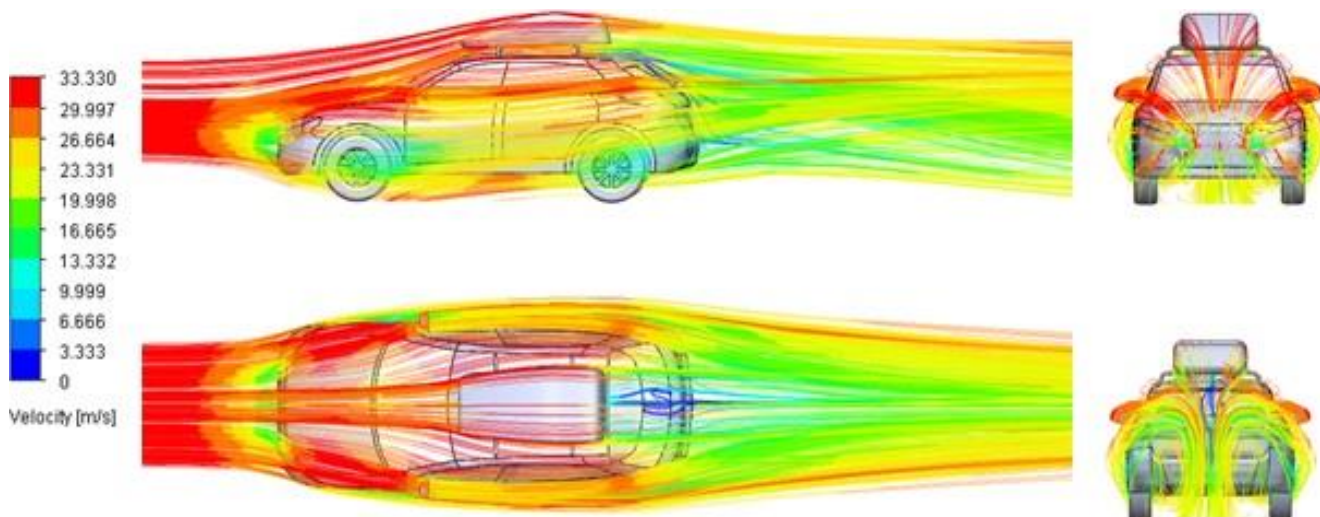
Figure 9. Visualization of air at 33.33 m/s velocity.
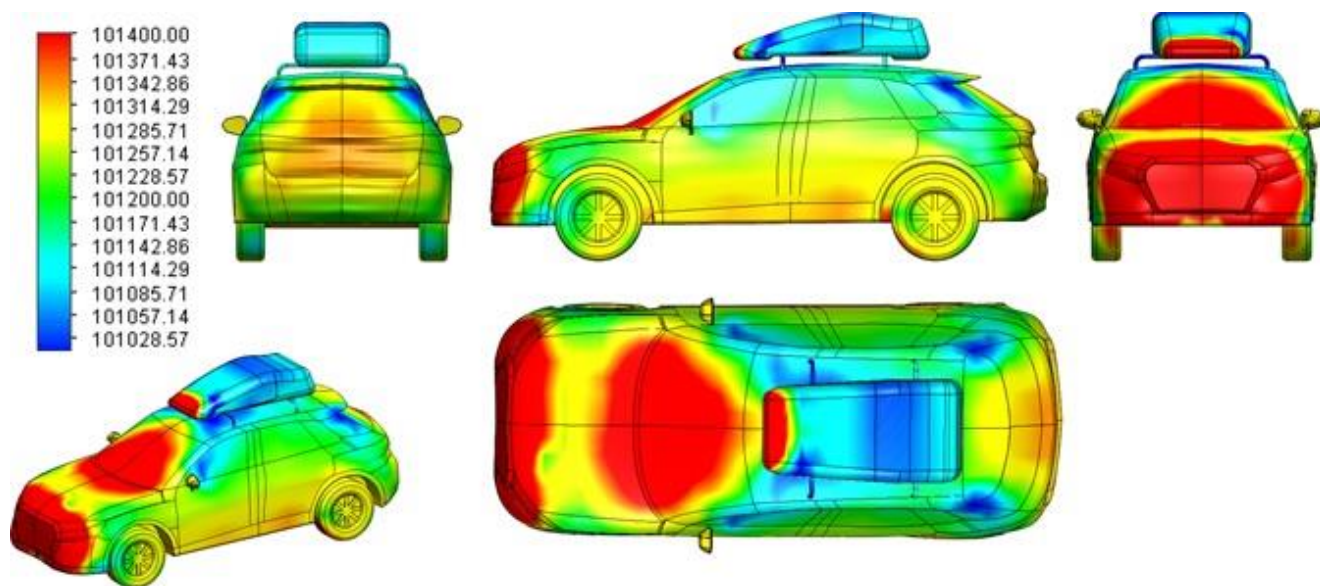
Figure 10. Visualization of the air pressure exerted on the vehicle surface and the luggage compartment

Table 2.
Compare the obtained CFD results

Car model without luggage compartment				Car model with luggage carrier	
Air velocity [km/h]	**Air velocity [m/s]**	**Drag force [N]**	**Drag coefficient**	**Drag force [N]**	**Drag coefficient**
40	11.11	68.4172	0.353	77.102	0.377
80	22.22	272.34	0.351	307.758	0.376
120	33.33	612.432	0.351	691.31	0.375
160	44.44	1089.72	0.352	1223.09	0.373
200	55.56	1700.63	0.352	1914.17	0.374

5. CONCLUSION

In this paper a comparative aerodynamic study is performed for two simulation cases at five different velocities. The software developed for simulating the airflow mechanical processes is an important future research of study for engineers, who can achieve in advance the optimal design of products, without additional costs of physical realization of a prototype. This study can be used to determine the aerodynamic geometry of the luggage carrier. The simulations performed prior to the vehicle design and manufacturing of the car must provide the manufacturing of a durable, high-performance and comfortable car. An additional disadvantage of using CFD calculation methods are highlighted by the training courses to learn of staff to be able to perform this analysis and the purchase price and maintenance of the software package.

REFERENCES

[1] Balcau M, Cristea AF. Theoretical considerations regarding the dynamic absorber. Acta Technica Napocensis-Series: Applied mathematics, mechanics, and engineering. 62(3), 2019

[2] Bodea, S-M., Prodan, C-V., Iacob-Liviu Scurtu, I-L., *The Aerodynamic Study of a Body Truck*, Proceedings of the 4th International Congress of Automotive and Transport Engineering (AMMA 2018), Proceedings in Automotive Engineering. Springer, https://doi.org/10.1007/978-3-319-94409-8_9, 2019

[3] Heft, A., Indinger, T., & Adams, N., *Introduction of a New Realistic Generic Car Model for Aerodynamic Investigations,* SAE 2012 World Congress, Detroit, Michigan, USA. Paper 2012-01-0168, https://doi.org/10.4271/2012-01-0168, 2012

[4] Huminic, A., Huminic, G., *Aerodynamics of curved underbody diffusers using CFD,* Journal of Wind Engineering and Industrial Aerodynamics, 205, 104300, https://doi.org/10.1016/j.jweia.2020.104300, 2020

[5] Janicki, R. M., & Piechna, A. *Examining influence of a rooftop cargo carrier position on automobile aerodynamics,* In AIP Conference Proceedings (Vol. 2078, No. 1, p. 020073). AIP Publishing LLC, https://doi.org/10.1063/1.5092076, 2019

[6] Latif, MF Abdul, et al., *Roof Box Shape Streamline Adaptation and the Impact towards Fuel Consumption,* MATEC Web of Conferences. Vol. 97. EDP Sciences,
DOI: 10.1051/matecconf/20179701089, 2017

[7] Saqr, K.M. and Musa, M.N., *RANS simulation of the turbulent flow field in the vicinity of the Ahmed reference car model,* New Aspects of Fluid Mechanics, Heat Transfer and Environment. Wseas, Taipi, pp.21-26, 2010

[8] Scurtu L., Borzan AI., Mariasiu F., Vlad N., Varga B., Morariu S. *Drag Coefficient Analysis for Side Mirrors of an Electric Vehicle Prototype,* In: Dumitru I., Covaciu D., Racila L., Rosca A. (eds) The 30th SIAR International Congress of Automotive and Transport Engineering. SMAT 2019. Springer, Cham. https://doi.org/10.1007/978-3-030-32564-0_57, 2020

[9] Scurtu, L. and Lupea, I., *Frontal crash simulation of a chassis frame,* Acta Tech. Napocensis, vol. 57(3), pp. 207–210, [Online]. Available: https://atna-mam.utcluj.ro/index.php/Acta/article/view/398 , 2014

[10] Scurtu L., Jurco A., Borza E.V., Mariasiu F., Vlad N., Morariu S. *Aerodynamic Study of an Electric Vehicle Prototype,* In: Dumitru I., Covaciu D., Racila L., Rosca A. (eds) The 30th SIAR International Congress of Automotive and Transport Engineering. SMAT 2019. Springer, Cham. https://doi.org/10.1007/978-3-030-32564-0_56, 2020

[12] Todoruţ, A., Cordoș, N., Burdea, M.D., Bălcău, Monica, *The evaluation of normal load redistribution on the static axles and on the wheels, when the vehicle is in motion*, ClujNapoca, Acta Technica Napocensis, Series: Applied Mathematics, Mechanics, and Engineering, Vol. 58(3), pg. 349-360, Ed. U.T.PRESS, ISSN 1221-5872, 2015

[13] Blueprints for 3D modelling, https://drawingdatabase.com/audi-q3-2018/

[14] SolidWorks, FlowWorks Help Files. 2020

THE MODELING AND SIMULATION OF PROPULSION SYSTEMS TO ESTIMATE CO$_2$ EMISSION

Cristian-Alexandru RENȚEA*, Gheorghe FRĂȚILĂ

POLITEHNICA University of Bucharest, Automotive Engineering Department,
Spl. Independenței, nr. 313, 060042, BUCHAREST, Romania

Abstract: *This paper aims to investigate the level of CO$_2$ emissions for the new test cycle - WLTC (Worldwide Harmonized Light Vehicles Test Cycle) considering two different gear shifting schedules. In order to underline the high level of trust of the models carried out, the obtained results are being compared for the CO$_2$ emissions obtained after simulation, and also through experimental investigation obtained on the rolling test bench.*

Key-Words: *WLTC, CO$_2$ emissions, engine temperature, simulation*

NOMENCLATURE

m : average vehicle speed, km/h
V : vehicle speed, km/h
VSF: vehicle speed fluctuation, %
σ : standard deviation of vehicle speed, km/h

1. INTRODUCTION

Since the new CAFE (Corporate Average Fuel Economy) regulations must be respected, in order for all types of car manufacturers to predict CO$_2$ emissions, the modelling and simulation of the propulsion systems is very important.

A model is a mathematical representation for the behavior of a process, a logic concept, or the operation of a system. The mathematical models of a dynamic system are mostly executed in numerical simulation environments. The purpose of a numerical simulation is to mimic the actual behavior of a system under controlled operating conditions. By analyzing the model predictions, one can improve the targeted aspects of the system in consideration [4].

The modelling process needs to sufficiently represent a target system for the purpose of simulating a model with specific predetermined experiments [3].

Nowadays, developing a product without simulation is inconceivable. Developing mathematical models which accurately describe physical phenomena, or the studied subsystems was made possible through the ever-increasing computing power, so that the projection and optimization decisions could be made in the early design stages, even before creating functional prototypes.

The CAFE regulations involve 30 to 40% reductions in CO$_2$ emissions from the 95 g/km level by 2021 [10]. Therefore, to avoid the penalties of hundreds of millions of euros, car manufacturers must develop the subsystems of the vehicle through which CO$_2$ emissions can be reduced. One of the most important subsystems of modern vehicles, even having the role of a command element for the internal combustion engine is the transmission.

To highlight the influence of manual transmission on CO$_2$ emissions using modelling and simulation, in this paper, the CO$_2$ emissions for two gear shift schedules, constructed in concordance to the regulation [8], will be estimated. The usual programs that can elaborate on such studies are AMESim, ADVISOR, Dymola, Easy5, SimulationX [1] [5].

---

* *Corresponding author e-mail:* rentea.cristian@yahoo.com

In order to simulate the CO_2 emissions of a vehicle, LMS Imagine.Lab AMESim, a modelling system and a simulation programming environment, is used in this paper. One of the main advantages is the library components availability, which can allow complex studies in most of the technical domains [2].

2. MODEL DEVELOPMENT

The complete model of the vehicle with conventional propulsion system able to follow test cycle (figure 1.) developed in LMS AMESim makes use of three libraries: IFP Drive, Mechanical and Signal & Control.
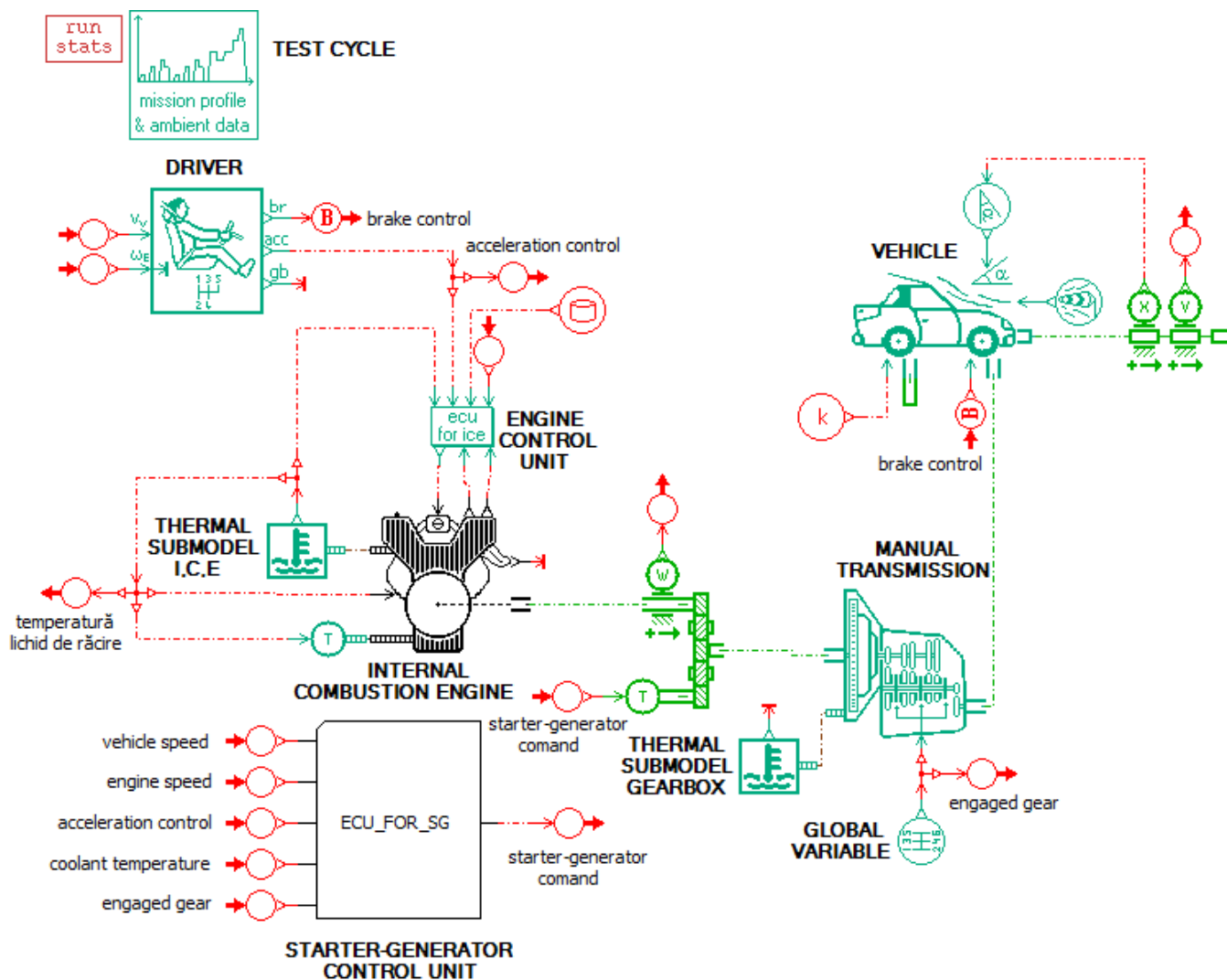

Figure 1. The vehicle model for estimating CO_2 emissions

The main submodels were extracted from the IFP Drive library and some of them are listed as follows: a driver submodel (DRVDRVA00A) necessary to follow the cycle given by the mission profile and ambient data submodel (DRVMP2A), internal combustion engine (DRVICE01E), engine control unit (DRVVECU1A), manual transmission with included clutch (DRVMGC01), two thermal submodels (DRVCOO0A), one for the internal combustion engine, and another for gearbox, utilized to compute engine and gearbox temperature, global variable (DRVGVS2A) and 1-D vehicle (DRVVEH4A).
A special component called "ECU_FOR_SG" (Electronic Control Unit for Starter-Generator) has been specially created to control the functioning for the Start&Stop systems.
The model can be considered of medium complexity, having 12 state variables.
The study is done for a class passenger car (SUV type) equipped with one-liter turbocharged gasoline engine with Start&Stop function and a 5 gears manual transmission.
The fuel consumption characteristics were determined experimentally.

3. RESULTS

After running the model, since a direct causal model is used, the first step is to check whether the vehicle speed falls within the speed limits (figure 2) determined according to the test regulations [9].

The first calibration applied to the model consists in the optimal choice of the fuel consumption coefficient for the cold start of the internal combustion engine. Using experimentally determined temperature curves, after several iterations, the model is calibrated in the domain of interest (where the temperature is below 50 °C), resulting a value of 1.74 for the coefficient.
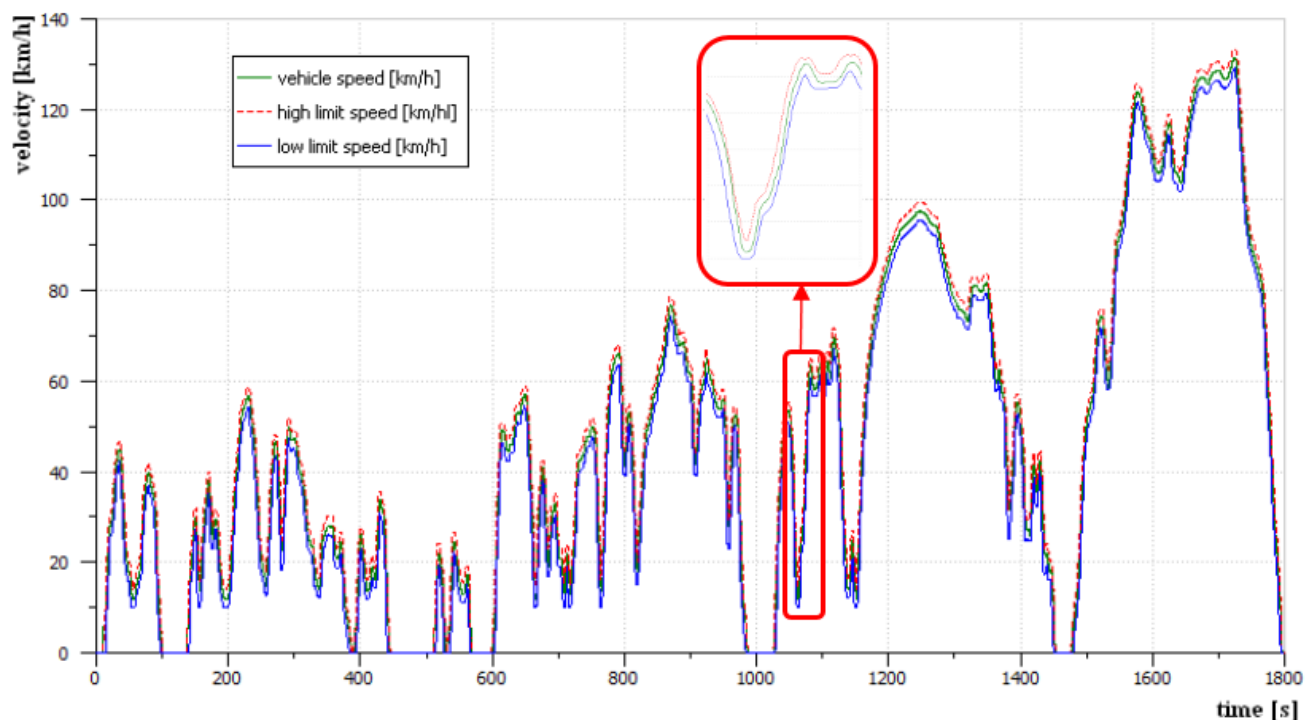

Figure 2. The variation of vehicle speed in relation to the required speed profile

The second calibration applied to the model is the calibration of the thermal submodels used to calculate the temperatures of the internal combustion engine and the gearbox, the temperature variation being shown in figure 3. The aim was to obtain a good correlation in the domain [0 ... 200] s, where the temperature varies strongly, having a major influence on CO_2 emissions.
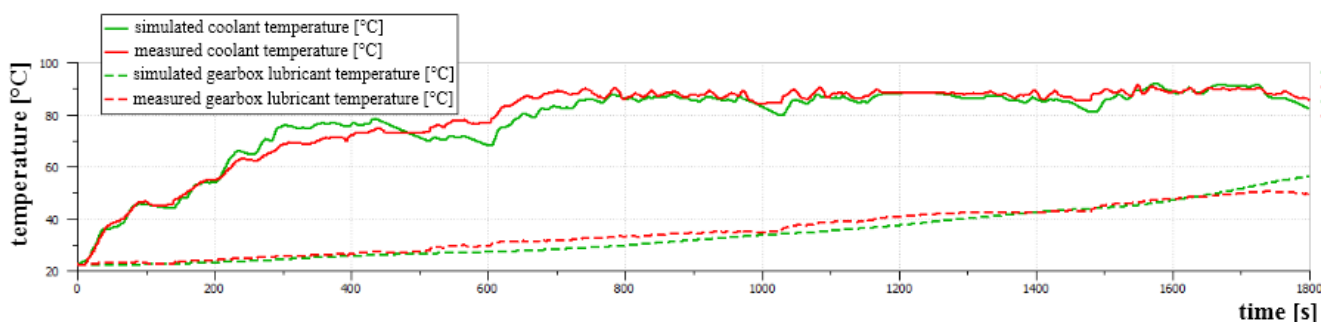
Figure 3. The variation of coolant and gearbox lubricant temperature during WLTC

The figures 4, 5, 6 and 7 show the variation of instantaneous and cumulative CO_2 emissions, obtained both in simulation and experimentally for the two tests [7]. From figures 4, 5, 6 and 7, one can remark a very good accuracy of the model developed in relation to the results obtained on the rolling test bench. Although the simulation showed that the CO_2 emissions for the whole cycle are close to those obtained experimentally with a relative error of 2.51% for test 1 and 3.7% for test 2, it is necessary to make an analysis of CO_2 emissions at each stage of the WLTC cycle given the different regimes at which the internal combustion engine operates.

Figure 4. The variation of instantaneous CO$_2$ emissions - test 1

Figure 5. The variation of cumulative CO$_2$ emissions - test 1

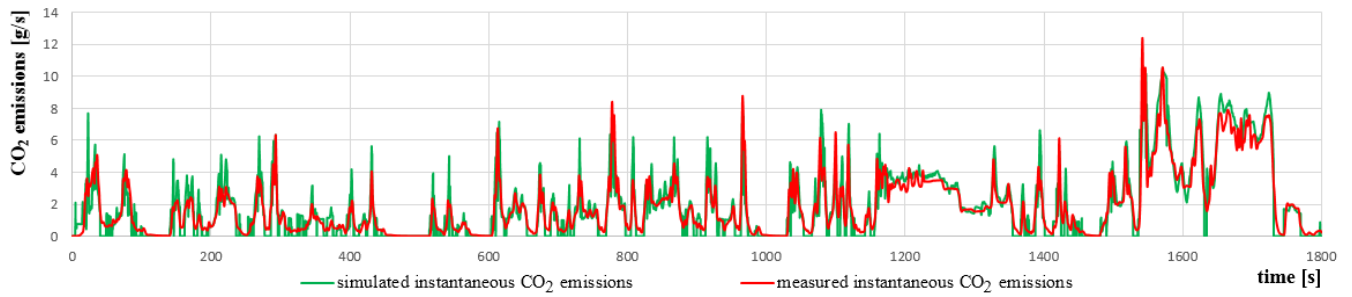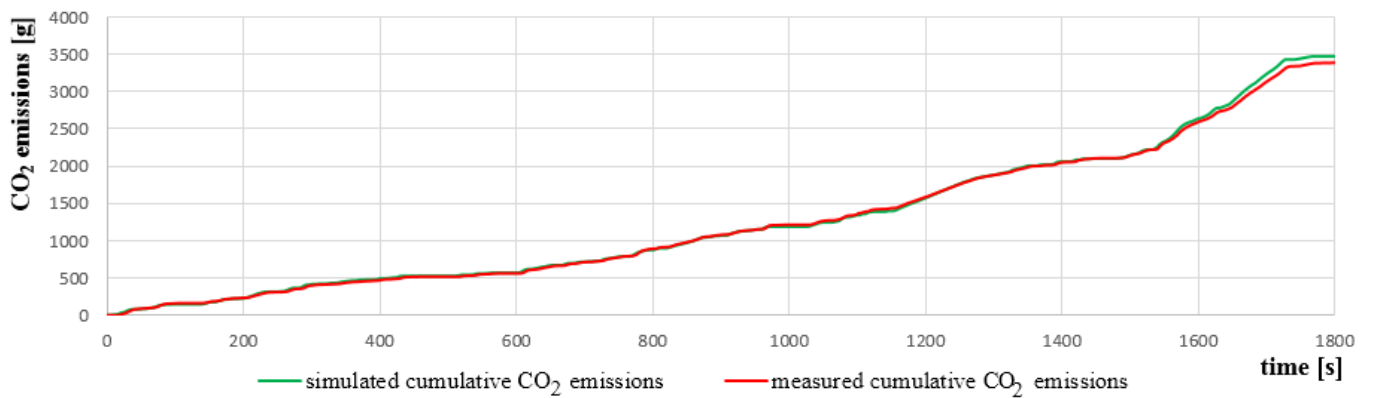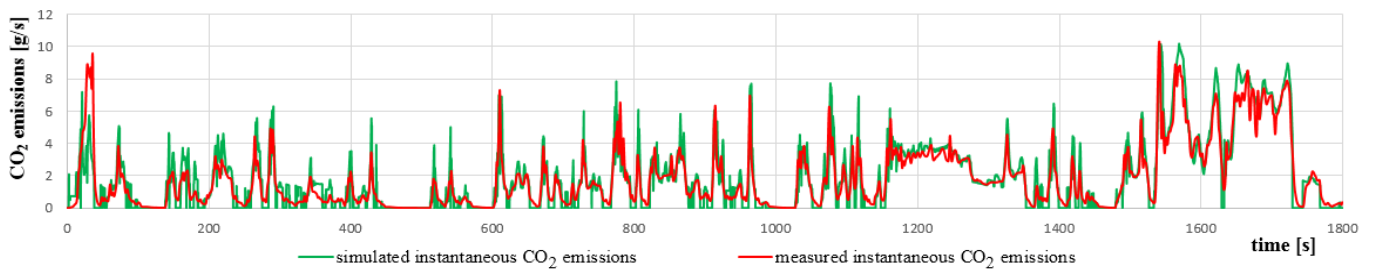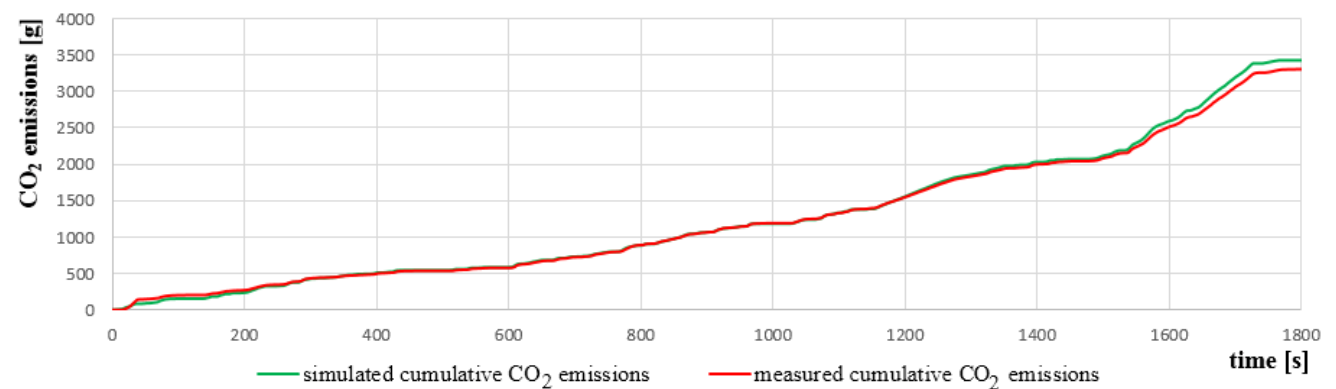*Figure 6. The variation of instantaneous CO$_2$ emissions - test 2*

Figure 7. The variation of cumulative CO$_2$ emissions - test 2

In order to quantify the fluctuation of vehicle speed in a test cycle, a specific parameter called VSF (Vehicle Speed Fluctuation) is defined in [6] as follows:

$$VSF = \frac{\sigma}{m} \cdot 100 \ [\%]$$

(1)

where: σ – standard deviation of vehicle speed; m – average vehicle speed.

Figure 8 shows the normal speed distribution and frequency of different speed values with a multiple of 10 km/h for the WLTC.
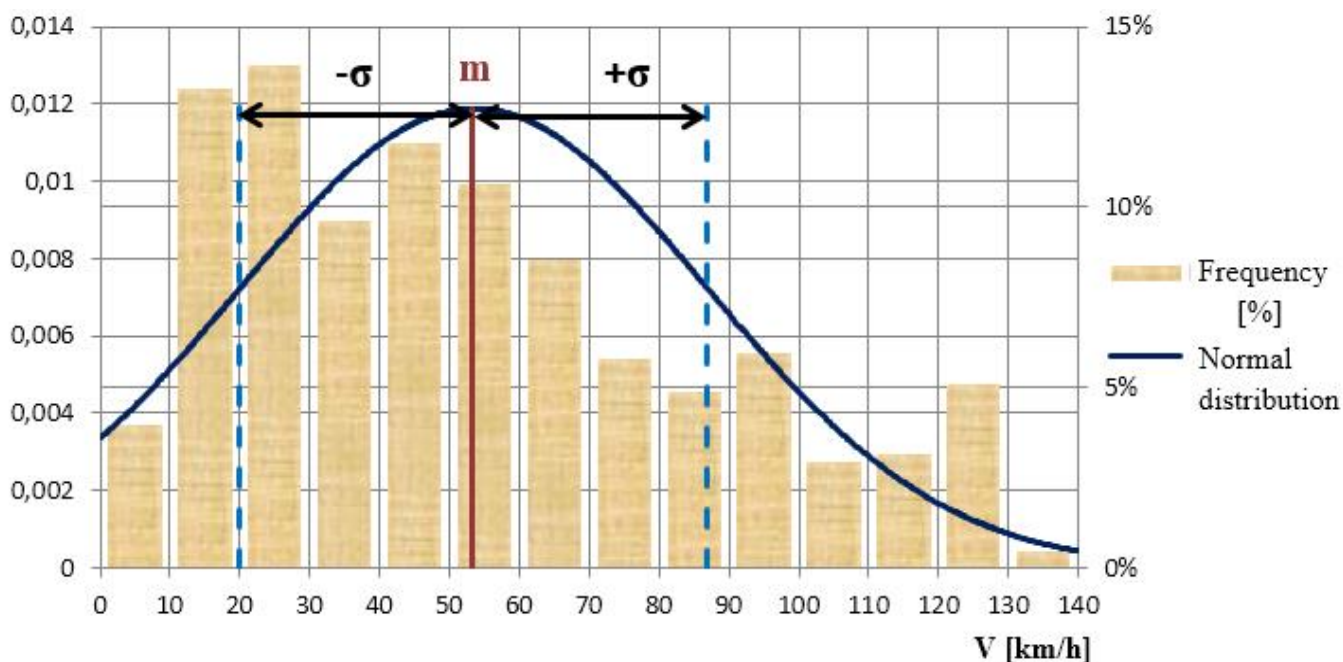
Figure 8. Normal speed distribution for the WLTC.

For a speed of between 120 and 130 km/h the occurrence frequency is approximately 5%, which shows that the gearbox upper gears are used more often than in the New European Driving Cycle (NEDC).
Table 1 presents the VSF values computed for each of the four phases of WLTC cycle. Also, in table 1 and in figures 9 and 10 the results obtained by both simulation and experimentally for each of the 4 phases of the cycle in the case of the two tests are presented. The relative error values (ε) for each phases of the cycle are also centralized.

Table 1.
Measured and simulated CO_2 emissions

Phase	VSF [%]	Test 1			Test 2		
		Simulated [g]	Measured [g]	$\|\varepsilon\|$ [%]	Simulated [g]	Measured [g]	$\|\varepsilon\|$ [%]
Low speed	51.5	569.12	562.39	1.20	585.45	577.56	1.37
Medium speed	39.3	608.14	650.57	6.52	586.50	612.82	4.30
High speed	43.2	890.21	894.10	0.43	862.47	852.50	1.17
Extra High speed	35.9	1326.53	1276.85	3.89	1315.61	1259.29	4.47
Total	62.8	3468.93	3383.91	2.51	3424.54	3302.17	3.70
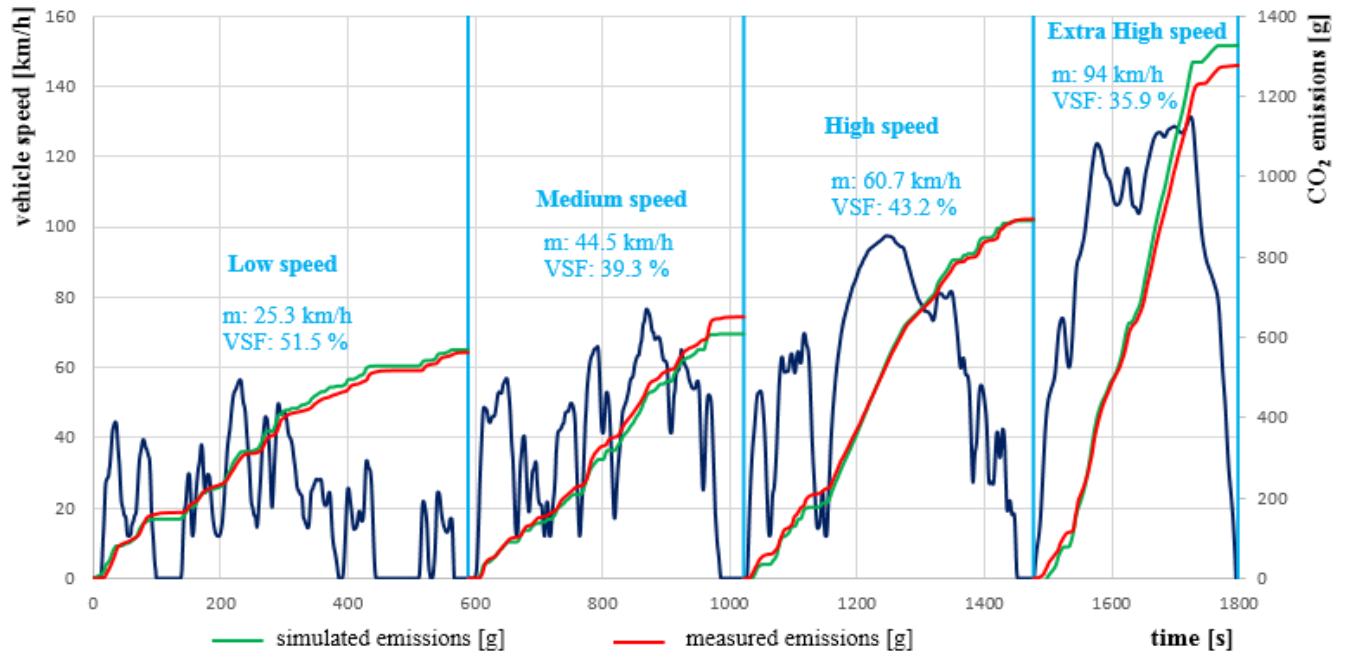
Figure 9. Cumulative CO$_2$ emissions at each phase – test 1
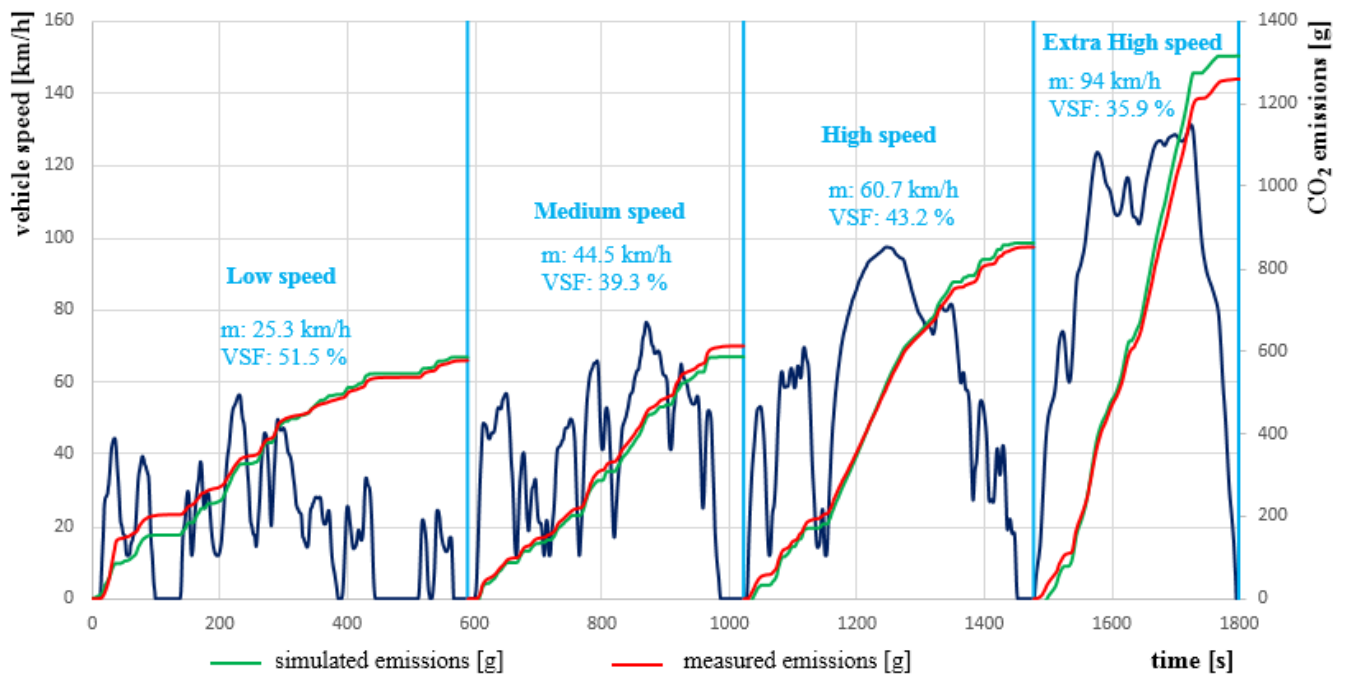
Figure 10. Cumulative CO$_2$ emissions at each phase – test 2

Analyzing table 1 and figures 9 and 10, it can be seen that the highest values for the relative error exceeding 5% are obtained in the phases of medium speed and extra high speed of the WLTC cycle, but through the whole cycle, the error is less than 4 %. It should also be noted that the values of the VSF parameter differ significantly from one phase of the WLTC cycle to another, varying between 35.9% and 51.5%, which highlight the high level of trust of the developed model.

Furthermore, it is desirable to evaluate the influence of the main factors which require additional modelling and calibration: coolant temperature and the Start&Stop system.

In this paper several simulations to highlight the influences are made.

For these simulations, one case implied that the internal combustion engine works at a nominal regime (the engine temperature is considered 90 °C) and a second case considers variable temperature.
Other simulations were done for the Start&Stop system being active.
The results obtained are presented in table 2.

Table 2.
CO_2 emissions obtained by simulation

Test	Phase	Engine thermal regime			Start & Stop		
		Variable [g]	Nominal [g]	$|\varepsilon|$ [%]	on [g]	off [g]	$|\varepsilon|$ [%]
1	Low speed	569.12	406.27	28.61	569.12	633.82	11.37
	Medium speed	619.21	598.56	3.33	619.21	638.86	3.17
	High speed	913.28	895.17	1.98	913.28	925.58	1.35
	Extra High speed	1367.33	1358.80	0.62	1367.33	1369.49	0.16
	Total	3468.93	3258.81	6.06	3468.93	3567.74	2.85
2	Low speed	585.46	415.33	29.06	585.46	647.36	10.57
	Medium speed	597.85	577.98	3.32	597.85	614.76	2.83
	High speed	885.44	867.52	2.02	885.44	895.45	1.13
	Extra High speed	1355.80	1347.36	0.62	1355.80	1357.93	0.16
	Total	3424.55	3208.19	6.32	3424.55	3515.49	2.66

From table 2, it can be stated that the engine thermal regime has a high influence on CO_2 emissions, the largest difference between the variable regime and the nominal regime being obtained during the initial phase (approx. 29%). Also, there is a maximum reduction of CO_2 emissions by activating the Start&Stop system is obtained in the low velocity phase (approx. 11%) and of roughly 3% for the whole WLTC cycle.

3. CONCLUSIONS

Modeling and simulation for the propulsion systems represent important means in terms of analyzing the CO_2 emissions. In this paper, it has been shown that precise models can be developed for conducting studies on the CO_2 emissions of the vehicle in a test cycle.
The developed model has a high level of trust, given that the VSF parameter values vary considerably between WLTC phases (from 35.9% to 51.5%).
In order to reduce the emissions for a manual transmission vehicle, it is recommended that the superior gears should be engaged, because of the high gear efficiency and its negligible variation with the torque and engine speed.
The consideration of the engine temperature's influence on CO_2 is more important compared with the Start&Stop system (in the low speed phase of the WLTC).
The cumulated effect can be observed in terms of CO_2 emissions by an increase of 6% over the values obtained at the nominal regime throughout the cycle.
On the other hand, activating the start&stop system implies a reduction of approximately 3% of CO_2 emissions over the entire WLTC cycle.

ACKNOWLEDGEMENT

REFERENCES

[1] Bătăuș, M. Dragne, F. Maciac, A. Oprean, M., Vasiliu N. *Models of Automotive Transmissions for Fuel Consumption Studies,* Proceedings of Advanced Transmission for Low CO_2 Vehicles, Paris: Institut Français du Pétrole, 2009

[2] Bătăuş, M. Vasiliu N. *Modelling of a Dual Clutch Transmission for Real Time Simulation*, UPB Sci. Bull. D 74 2 p 251, 2012

[3] Gao, W., Chris, Mi., Emadi, A. *Modeling and Simulation of Electric and Hybrid Vehicles*, Proceedings of the IEEE, SUA, vol. 95, 2007

[4] Koprubasi, K. *Modeling and Control of a Hybrid-Electric Vehicle for Drivability and Fuel Economy Improvements,* The Ohio State University, 2008

[5] Lontis, N. S., Mihon, N., Vetres, I. *Numerical simulation study of a hybrid road vehicle regarding fuel economy and ambient emission delivery*, Romanian Journal of Automotive Engineering, vol. 23, no.2, June, 2017

[6] Oota Y. *The advantage of CVT in the real word,* 12th International CTI Symposium, Berlin, 2013

[7] Renţea, C. *Cercetări privind influenţa transmisiei asupra consumului energetic al automobilului,* Teză de doctorat, UPB, 2021

[8] COMMISSION REGULATION (EU) 2018/1832 of 5 November 2018 amending Directive 2007/46/EC of the European Parliament and of the Council, Commission Regulation (EC) No 692/2008 and Commission Regulation (EU) 2017/1151 for the purpose of improving the emission type approval tests and procedures for light passenger and commercial vehicles, including those for in-service conformity and real-driving emissions and introducing devices for monitoring the consumption of fuel and electric energy

[9] COMMISSION REGULATION (EU) 2017/1151 of 1 June 2017 supplementing Regulation (EC) No 715/2007 of the European Parliament and of the Council on type-approval of motor vehicles with respect to emissions from light passenger and commercial vehicles (Euro 5 and Euro 6) and on access to vehicle repair and maintenance information, amending Directive 2007/46/EC of the European Parliament and of the Council, Commission Regulation (EC) No 692/2008 and Commission Regulation (EU) No 1230/2012 and repealing Commission Regulation (EC) No 692/2008

[10] *** www.auto-infos.fr, accessed in 17 november 2020

AERODYNAMIC STUDY OF A CAR TOWING A MOTOCYCLE TRAILER

Monica BALCAU[*]

Technical University of Cluj-Napoca, Department of Automotive Engineering and Transports,
Bulevardul Muncii 103-105, 400641 CLUJ-NAPOCA, Romania

Abstract: In this paper is presented a comparative aerodynamic study of a generic vehicle geometry for two cases: in the first case are calculated the aerodynamic force and coefficient of the vehicle body, and in the second case where the vehicle is towing a trailer with motorcycle. The first part of the paper presented some studies regarding the actual computerized CFD simulation method used in automotive industry. In the second part of the paper the CAD modelling methodology of the vehicle body and the trailer with the motorcycle are presented. The vehicle and the trailer with motorcycle geometry are simulated at six different airflow velocity establishing the aerodynamic force and drag coefficient. The interpretation of the results and conclusions of this aerodynamic study are presented in the last part of the paper, where can be observed the behavior of the air streamlines around the vehicle body.

Key-Words: Aerodynamic evaluation, Drag force, CFD process, CAD modelling

1. INTRODUCTION

Nowadays, the aerodynamic efficiency in modern automotive fabrication is the important factor which have an influence on the performance and fuel consumption. By using the CAD design, crash simulation and CFD simulation software, the optimal shape of the car body can be determined from the design stage [6]. An important recent study is performed for Ahmed body shape with the underbody diffuser and variable rounded inlet section. The influence of the diffuser on drag and lift for five length of the diffuser, each of them for the different angle: 1°, 3°, 5°, 7°, 9° are simulated. The CFD software used was ANSYS CFX -12.0 and the surface of the Ahmed body reference model for 35° angle of the rear side and the simple underbody was modelled as a parametrized CAD model into the design module [3]. Another aerodynamic study presents the numerical evaluation of the used Reynolds Averaged Navier-Stokes (RANS) models and Detached Eddy Simulation (DES) models of a passenger vehicle with two front bumper models comparing with DES method. The car surface was meshed in ANSA and Nastran software, after the model is simulated into a Star CCM+ commercial CFD code. After simulation is observed that using the DES model the prediction of the drag coefficient not showing superior performance over using RANS model, but DES method is able to predict the higher fidelity of the fluid flow [9]. The comparative study to determine the aerodynamic under the wind effect are achieved for a baseline SUV vehicle in two body shape variants: first variant the square back and the second the notchback. After simulation can be observed that the air turbulence created by the wind has a negative influence to establish the SUV vehicle aerodynamics. The sedan shapes may be less sensitive to wind conditions than the SUV geometry vehicles [2]. The aerodynamic study of a truck structure using the CFD simulation method is performed in the FlowWorks module integrated in SolidWorks software. A comparison study is made between the basic model of a truck and the improved model that contains air deflectors, mounted to obtain a lower aerodynamic force and implicitly a better aerodynamic coefficient [1]. The CFD simulation of the truck structure is performed at a velocity of 25 m/s for both cases. After interpreting the obtained results, the improved truck model with air deflectors has a lower aerodynamic coefficient by 0.13 compared to the base truck model. Also, an auxiliary equipment of the car which can affect its aerodynamics are the side mirrors. The aerodynamic performance of a car is affected by the side mirrors geometry in a proportion of approximately 2-5 % [4].

---

[*] *Corresponding author e-mail:* monica.balcau@auto.utcluj.ro

A CFD study conducted to determine an optimal body structure is presented by Scurtu and authors, where the value of the aerodynamic coefficient and the aerodynamic force for an EV prototype car body is determined. The simulation is performed at four speed cases: 14 m/s, 25 m/s, 34 m/s and 55 m/s. The values of calculated aerodynamic coefficient for each simulation case are situated in the range 0.28-0.29 [5]. The aerodynamic study of this paper was done to see the aerodynamic influence while using the trailer for transporting motorcycles attached to a SUV vehicle. To observe the differences, two simulation cases are performed: first simulation case that includes only the car model and the second case that includes the SUV vehicle that towing a motorcycle trailer. The idea of this study is materialized to determine the future of an aerodynamic structure of a trailer for transporting motorcycles. Due to inexistent aerodynamic studies that show the aerodynamic evaluation of the actual SUV vehicle that towing a motorcycle trailer this study may be the first step in determining a new aerodynamic trailer structure.

2. CFD APPLICATION

The airflow around the car body while driving on the road present a complex simualtion process. An important factor to the generate of an aerodynamic body model is represented by the designer's experience in generating the aerodynamic body models. The aerodynamic study described in present paper is based on the application of the CFD simulation method to evaluate the car body aerodynamics. In figure 1 is presented the necessary steps to follow to achieve a CFD simulation, starting with the realization of an CAD model and after it is included into a fluid simulation software environment, followed by the creation of the computational domain meshed with finite elements.
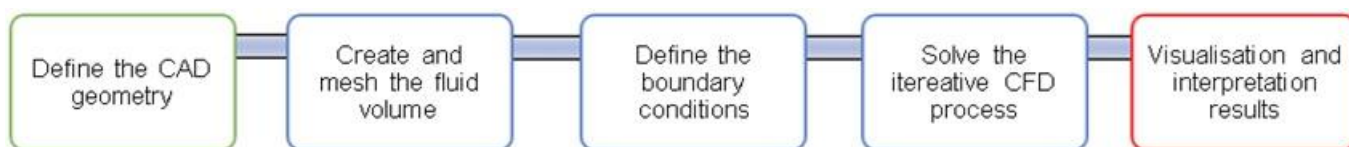

Figure 1. CFD simulation steps

By define the boundary conditions the user can add different fluid mechanical properties and the value of the fluid velocity flow is set. The final step of the CFD simulation is given by the visualization and interpretation of the obtained results. The method and work steps of the CFD simulations performed in this study are detailed during the paper for a better understanding of the process.

2.1 CAD model design
The geometry of the vehicle body is approximately elaborated by the shape of the BMW X1 car model using blueprint photos method in the SolidWorks modeling environment, as can be seen in figure 2a, [11].
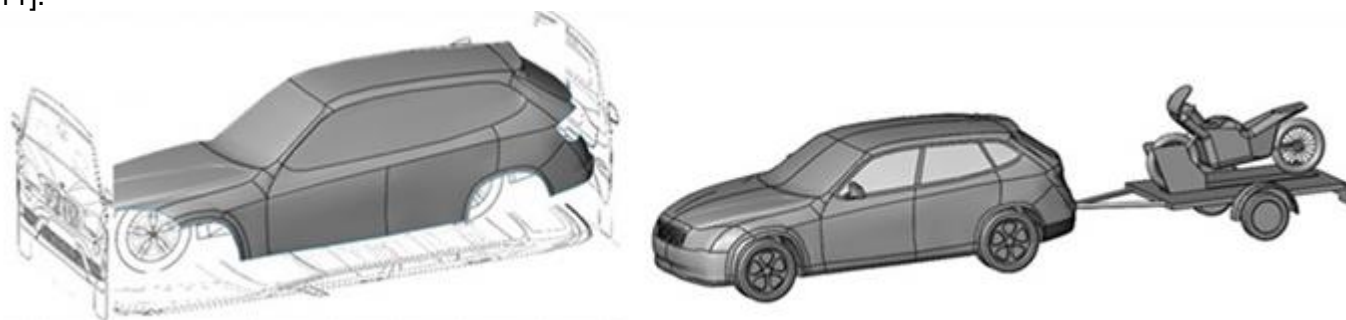
a) Design the CAD model of the car body   *b) Final CAD model*
Figure 2. CAD model of the car body

The CAD modeling was done in two stages: in the first stage of modeling the car model was designed, and in the second stage the generic model of the motorcycle and the trailer was modeled, as can be seen in figure 2b. The overall dimensions of the CAD models designed in this study are in concordance with the real motorcycle and trailer models.

By following the modelling process, the resulting car model is represented in figure 3 in which the final shape and overall dimensions can be observed. For the geometry of the car to be as comparable as possible with the real car, the wheels housings, rims, mirrors, and other details related were modeled in detail.
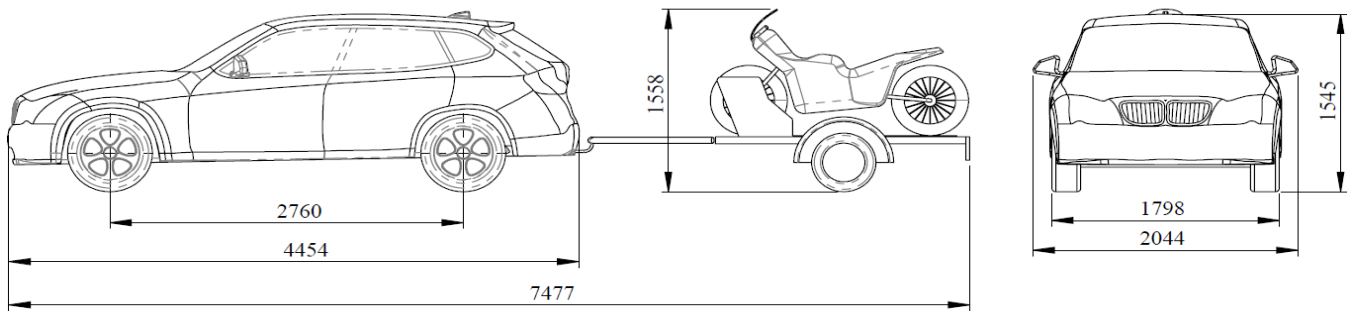

Figure 3. The overall dimensions of the CAD model

The SUV geometry is designed with the closed radiator grille, there is no airflow in the engine compartment, and no wipers are mounted on the windshield surface. The exterior details of the SUV body, trailer, and motorcycle model were reproduced as best as possible to obtain the most accurate results.

2.2 Computational domain creation and meshing of the fluid volume

This stage involves the inserting of the car model into a computational domain with a width of 4 m, a height of 3 m and a length of 25 m, presented in figure 4. The length of the CFD domain is established to observe the effects of air flow over the car geometry. In case of the first simulation case, the domain is discretized into 2568 fluid elements, of which 3157 met the surface of the model and in the second simulation case with trailer and motorcycle the domain is discretized into 33988 fluid elements, of which 5605 come into contact whit the model surface. Also, the number of discretization layers is higher near the model surface, as can be seen the mesh detail from figure 4, in order to have a higher accuracy of the results. The air inlet is positioned at the 5 m in front of the body car to view the air streamline behavior in the simulation process.
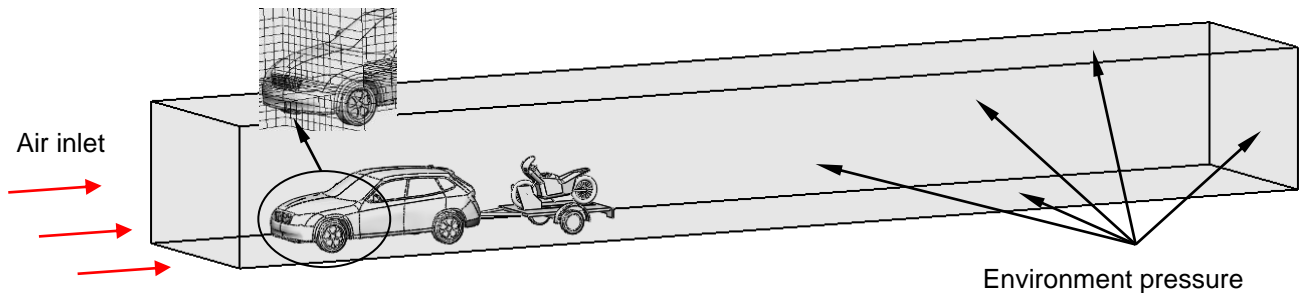

Figure 4. Computational domain and mesh detail

2.3 Boundary conditions

An important aspect is given by establishing if the air flow regime is laminar or turbulent. This aspect it can be determined by the Reynolds number that gives a measure of the ratio of inertial forces to viscous forces [7]. The expression of the Reynolds number is defined in relation 1.

$$R_e = \frac{\rho V L}{\mu} \tag{1}$$

Where,
μ: dynamic viscosity of the air free stream, kg/m·s
L: length of the vehicle model, m
ρ : air density, kg/m^3
V : air velocity, m/s

The values of the Reynolds number are calculated in Table 1 for all six reference velocity cases for model without the trailer with motorcycle simulated in this paper at the atmospheric air density ρ=1.225 kg/m³ corresponding at 15 °C temperature, dynamic viscosity of the air μ=1.802x10⁵ and the length of the vehicle model L=4.454 m.

Table 1.
Reynolds number values for reference velocity

Velocity [m/s]	16.67	25	33.33	41.67	50	58.33
R_e	5.047x10⁶	7.57x10⁶	1.009x10⁷	1.262x10⁷	1.514x10⁷	1.766x10⁷

The resulted values of the Reynolds number describe the turbulent flow dominated by the inertial forces, which led to produce vortices or flow instability. Generally, the typical values of the Reynolds number for the passenger car are of the order of 10^7 [7]. On the vehicle act forces that appear due to its advance through the air volume and forces that appear due to the mechanical effects produced by the vehicle components. A detailed study that determines the forces acting on the car during movement is presented by Todorut and authors [8]. The expression of the aerodynamic force is presented in relation 2 [1].

$$F_x = \frac{1}{2} \cdot \rho \cdot V^2 \cdot C_D \cdot A \tag{2}$$

Where,
ρ : air density
V : air velocity
C_D : aerodynamic coefficient
A : frontal area of the car
From relation 2 results the expression of the aerodynamic coefficient which is presented in relation 3. The frontal area of the car body surface used to determine the aerodynamic coefficient is measured into the modelling software and is equal to 2.65 m².

$$C_D = \frac{2 \cdot F_x}{\rho \cdot V^2 \cdot A} \tag{3}$$

2.4 Solving the CFD process

This stage is one of the most important stages of the CFD simulation process. The software module that allows solving this step is called *"solver"* and is intended to solve systems of basic equations that describe the CFD process algorithm [10]. In this study the CFD simulation were performed on an HP Z400 graphics station with a 3 GHz operating frequency Intel Xeon processor, 16 GB of RAM and a 1 GB Nvidia Quadro FX 3800 graphics card.
The governing equations used in this CFD simulation are the Reynolds-Averaged Navier-Stokes (RANS) equations in their conservation form [3]. The equilibrium RANS equations for incompressible, viscous and isothermal flow of a Newtonian fluid in cartesian coordinates given in differential equation and conservation form are presented in relations 4 and 5 in the Boussinesq's hypothesis:

$$\frac{\partial v_i}{\partial x_i} = 0 \tag{4}$$

$$\rho_\infty = \frac{\partial v_i v_j}{\partial x_j} = -\frac{\partial p}{\partial x_i} + \frac{\partial}{\partial x_j} \mu_\infty \left(\frac{\partial v_i}{\partial x_j} + \frac{\partial v_j}{\partial x_i} \right) - \rho_\infty \frac{\partial}{\partial x_j} \left(v_i' v_j' \right) \tag{5}$$

Where,
x_i, x_i : cartesian coordinates

$v_i^{'}, v_j^{'}$: parts of the fluctuating velocity

p: average pressure

ρ_∞ : constant density of the free air stream

μ_∞ : constant dynamic viscosity of the air free stream

The turbulent Reynolds stress tensor $\overline{v_i^{'}v_j^{'}}$ is presented in equation 6, where is modelled by Boussinesq's hypothesis [3].

$$\overline{v_i^{'}v_j^{'}} = -\frac{\mu_t}{\rho}\left(\frac{\partial v_i}{\partial x_j} + \frac{\partial v_j}{\partial x_i}\right) + \frac{2}{3}k\delta_{ij}$$

(6)

Where,

μ_t : turbulent viscosity

δ_{ij} : Kroneker delta: $\delta_{ij}=1$ if i=1 and $\delta_{ij}=0$ if $i \neq 1$

The expresion of the turbulence kinetic energy is given in relation 7:

$$k = \frac{\overline{v_i^{'}v_j^{'}}}{2}$$

(7)

Closing the system of equations is done with the turbulent model Shear-Stress-Transport (SST) developed by Menter that is based on the Willkox model [3].

2.5 CFD results

The last stage of the CFD simulation process is the visualization and interpretation the numerical results obtained for each of the six cases. In the visualization mode present within the software, is also the possibility of making animations of the fluid interaction process with the model geometry.

2.5.1 Simulation results for car model without trailer
The pressure exerted on the model is represented in figure 5, where it can be seen that the maximum air pressure is exerted in the front of the car on the bumper area, hood, and windshield. The airflow streamline resulted of the simulation at 50 m/s velocity are presented in figure 6, where it can be seen that in the rear side of the car body and in the area of the wheels housing have a high turbulent flow compared to the external car surface.
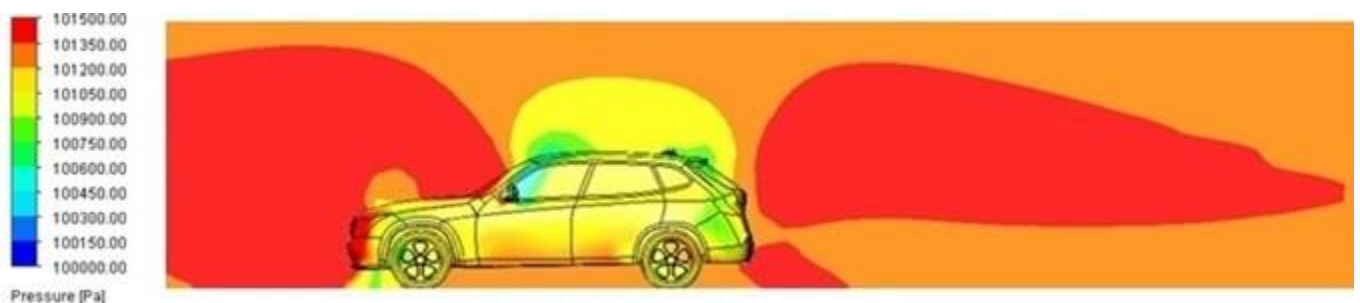

Figure 5. Pressure distribution on the model surface

2.5.2 Simulation results for the car towing a motorcycle trailer
In figure 7 in addition to the pressure exerted on the surface of the vehicle body, there is also air pressure on the motorcycle and the trailer surface, which will increase the value of the aerodynamic force. The distribution of streamline shown in figure 8 shows a sudden flow velocity decrease when the air reaches the surface of the motorcycle, generating turbulence flow. The numerical results of the drag force and drag coefficient obtained for each case, at different simulation speeds are presented in table 2 for the simulation of the vehicle without trailer and in table 3 for the vehicle with trailer.
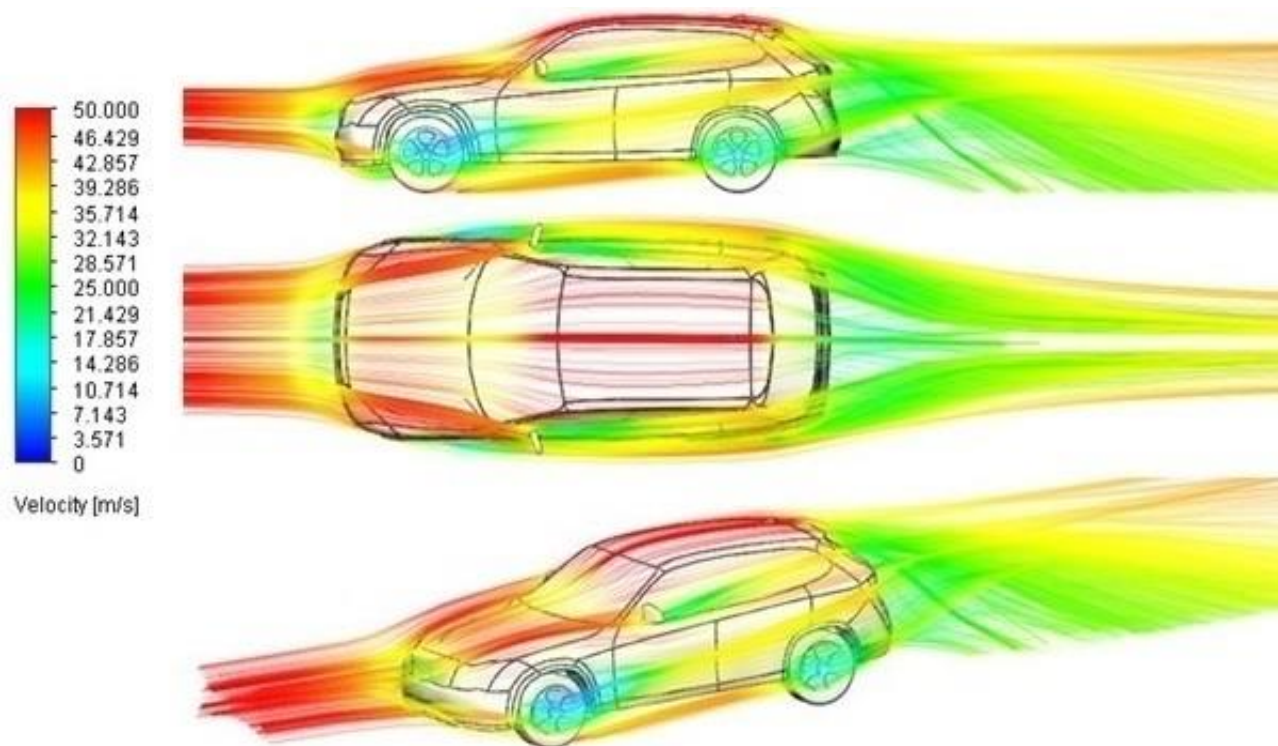
Figure 6. Distribution of flow lines around the car

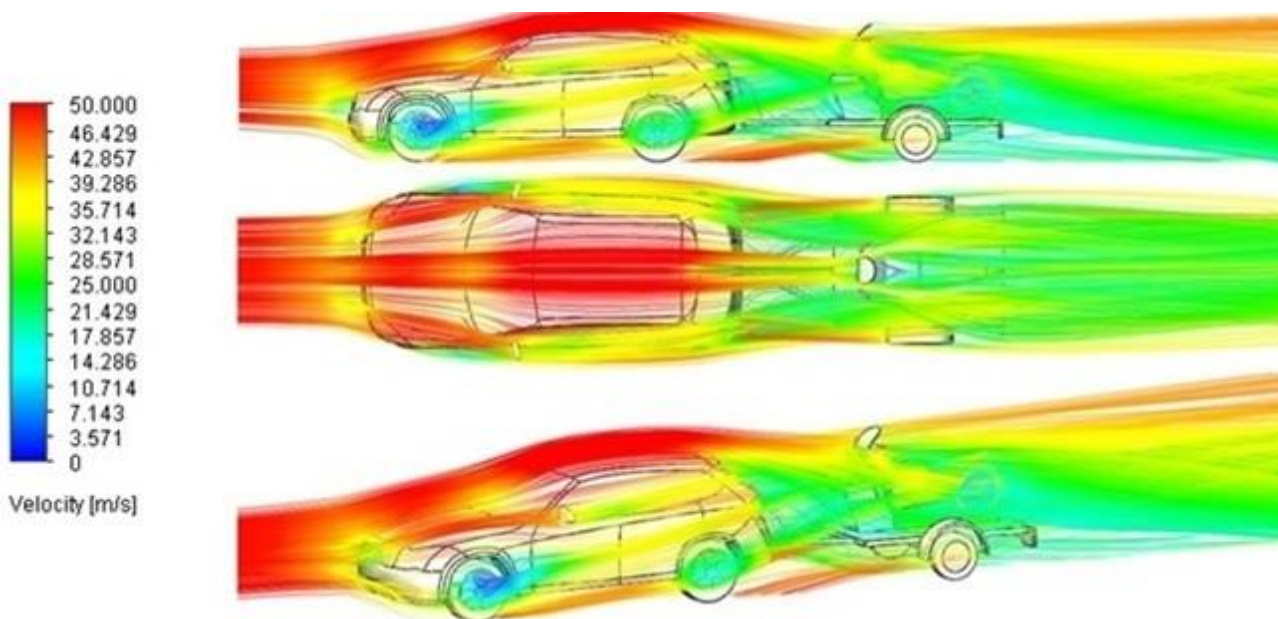*Figure 7. Pressure distribution on the model surface with the trailer and motorcycle*

Figure 8. Air flow at 50 m/s velocity

Table 2.
Results obtained for the first model simulation

Velocity [m/s]	Drag Force [N]	Drag coefficient
16.67	158.35	0.356
25	358.68	0.359
33.33	636.84	0.359
41.67	1005.09	0.362
50	1450.38	0.363
58.33	1973.72	0.363

Analyzing the obtained results for simulation cases at different flow velocity, can be observed that the aerodynamic force for the model without trailer is in the range 158.35 - 1973.72, and in the model with trailer and motorcycle is in the range 192.38 - 2356.88. In the second case the aerodynamic force is higher than in the first case, as well as the aerodynamic coefficient increases in the case of towing the motorcycle trailer, as can be seen in table 3.

Table 3.
Results obtained for the second model simulation

Velocity [m/s]	Drag Force [N]	Drag coefficient
16.67	192.38	0.433
25	435.87	0.435
33.33	775.48	0.437
41.67	1208.29	0.435
50	1735.32	0.435
58.33	2356.88	0.434

3. CONCLUSION

In present paper, a CFD study was performed to evaluate the aerodynamic performance for an existing SUV car body used in two cases at different driving velocity: the case of driving the car on the road and the second case in which it tows a trailer on which a motorcycle is placed. In order to carry out this study, the software necessary for the CAD realization of the car and the module with the calculation tools within it were used. Comparing the result for both simulation cases can be observed that in both cases the drag coefficient remains approximately constant. The CFD software applications used before the design process and manufacturing to determine the flow of fluids is useful to determine the optimal shape of the product, it is not necessary to make a physical prototype.

REFERENCES

[1] Bodea, S-M., Prodan, C-V., Scurtu, I-L., *The Aerodynamic Study of a Body Truck*, Proceedings of the 4th International Congress of Automotive and Transport Engineering (AMMA 2018), Proceedings in Automotive Engineering. Springer, Cham. https://doi.org/10.1007/978-3-319-94409-8_9, 2019
[2] Duncan, B., D'Alessio, L., Gargoloff, J. and Alajbegovic, A., *Vehicle aerodynamics impact of on-road turbulence. Proceedings of the Institution of Mechanical Engineers,* Part D: Journal of Automobile Engineering, 231(9), pp.1148-1159, 2017
[3] Huminic, A., Huminic, G. and Soica, A., *Study of aerodynamics for a simplified car model with the underbody shaped as a Venturi nozzle,* International journal of vehicle design, 58(1), pp.15-32, 2012.
[4] Scurtu L., Borzan AI., Mariasiu F., Vlad N., Varga B., Morariu S. *Drag Coefficient Analysis for Side Mirrors of an Electric Vehicle Prototype,* In: Dumitru I., Covaciu D., Racila L., Rosca A. (eds) The 30th SIAR International Congress of Automotive and Transport Engineering. SMAT 2019. Springer, Cham. https://doi.org/10.1007/978-3-030-32564-0_57, 2020

[5] Scurtu L., Jurco A., Borza E.V., Mariasiu F., Vlad N., Morariu S. *Aerodynamic Study of an Electric Vehicle Prototype,* In: Dumitru I., Covaciu D., Racila L., Rosca A. (eds) The 30th SIAR International Congress of Automotive and Transport Engineering. SMAT 2019. Springer, Cham. https://doi.org/10.1007/978-3-030-32564-0_56, 2020

[6]Scurtu, L. and Lupea, I., *Frontal crash simulation of a chassis frame,* Acta Tech. Napocensis, vol. 57(3), pp. 207–210, [Online]. Available: https://atna-mam.utcluj.ro/index.php/Acta/article/view/398, 2014

[7] Sebben, S., Walker, T. and Landström, C. *Fundamentals, Basic Principles in Road Vehicle Aerodynamics and Design,* Encyclopedia of Automotive Engineering, pp.1-16, 2014

[8] Todoruţ, A., Cordoș, N., Burdea, M.D., Bălcău, Monica, *The evaluation of normal load redistribution on the static axles and on the wheels, when the vehicle is in motion*, Cluj-Napoca, Acta Technica Napocensis, Series: Applied Mathematics, Mechanics, and Engineering, Vol. 58(3), pg. 349-360, Ed. U.T.PRESS, ISSN 1221-5872, 2015

[9] Zhang, C., Bounds, C.P., Foster, L. and Uddin, M., *Turbulence Modeling Effects on the CFD Predictions of Flow over a Detailed Full-Scale Sedan Vehicle,* Fluids, *4*(3), p.148, 2019

[10] Solidworks software, Help Files, 2018

[11] https://drawingdatabase.com/bmw-x1-2012/, 2020

AIMS AND SCOPE

The Romanian Journal of Automotive Engineering has as its main objective the publication and dissemination of original research in all fields of „Automotive Technology, Science and Engineering". It fosters thus the exchange of ideas among researchers in different parts of the world and also among researchers who emphasize different aspects regarding the basis and applications of the field.

Standing as it does at the cross-roads of Physics, Chemistry, Mechanics, Engineering Design and Materials Sciences, automotive engineering is experiencing considerable growth as a result of recent technological advances. The Romanian Journal of Automotive Engineering, by providing an international medium of communication, is encouraging this growth and is encompassing all aspects of the field from thermal engineering, flow analysis, structural analysis, modal analysis, control, vehicular electronics, mechatronics, electro-mechanical engineering, optimum design methods, ITS, and recycling. Interest extends from the basic science to technology applications with analytical, experimental and numerical studies.

The emphasis is placed on contribution that appears to be of permanent interest to research workers and engineers in the field. If furthering knowledge in the area of principal concern of the Journal, papers of primary interest to the innovative disciplines of „Automotive Technology, Science and Engineering" may be published.
No length limitations for contributions are set, but only concisely written papers are published. Brief articles are considered on the basis of technical merit. Discussions of previously published papers are welcome.

Notes for contributors
Authors should submit an electronic file of their contribution to the **Production office:** www. siar.ro. All the papers will be reviewed and assessed by a series of independent referees.

Copyright
A copyright transfer form will be send to the author. All authors must sign the "Transfer of Copyright" agreement before the article can be published.

Upon acceptance of an article by the journal, the author(s) will be asked to transfer copyright of the article to the publisher. The transfer will ensure the widest possible dissemination of information. This Journal and the individual contributions contained in it are protected by the copyright of the SIAR, and the following terms and conditions apply to their use:

The Scientific Journal of SIAR
A Short History

The engineering of vehicles represents the engine of the global development of the economy.

SIAR tracks the progress of the automotive engineering in Romania by: the development of automotive engineering, the development of technologies, and road transport services; supporting the work of the haulers, supporting the technical inspection and of the garage; encouraging young people to have a career in the automotive engineering and road haulage; stimulation and coordination of activities that promote an environment that is suitable for continuous education and improving of knowledge of the engineers; active exchange of ideas and experience, in particular for students, master students, PhD students, and young engineers, and dissemination of knowledge in the field of automotive engineering; cooperation with other technical and scientific organizations, employers' and socio-professional associations through organization of joint actions, of mutual interest.

By the accession to FISITA (International Federation of Automotive Engineering Societies) since its establishment, SIAR has been involved in achieving an overall professional community that is homogeneous in competence and performance, interactive, dynamic, and competitive at the same time, oriented towards a balanced and friendly relationship between people and the environment; this action will be constituted as a challenge worthy of effort and recognition.

The insurance of a favorable framework for the initiation and the development of cooperation of the specialists in this field of activity allows for an efficient and easy exchange of information, specific knowledge and experience; it supports the cooperation between universities and between research centers and industry; it speeds up the process of implementing the new technologies, it simplifies the identification of training and specialization needs of the personnel involved in the engineering of motor vehicles, transport, and road safety.

In order to succeed, ever since its founding, SIAR has considered that the stress should be put on the production and distribution, at national and international level, of a publication of scientific quality.

Under these circumstances, the development of the scientific magazine of SIAR had the following evolution:

1. RIA – Revista inginerilor de automobile (in English: *Journal of Automotive Engineers*)
ISSN 1222 – 5142

Period of publication: 1990 – 2000	Format: print, Romanian
Frequency: Quarterly	Electronic publication on: www.ro-jae.ro
Total number of issues: 30	Type: Open Access

The above constitutes series nr. 1 of SIAR scientific magazine.

2. Ingineria automobilului (in English: *Automotive Engineering*)
ISSN 1842 – 4074

Period of publication: as of 2006	Format: print and online, Romanian
Frequency: Quarterly	Electronic publication on: www.ingineria-automobilului.ro
Total number of issues: 58	Type: Open Access
(including the March 2021 issue)	

The above constitutes series nr. 2 of SIAR scientific magazine (Romanian version).

3. Ingineria automobilului (in English: *Automotive Engineering*)
ISSN 2284 – 5690

Period of publication: 2011 – 2014	Format: online, English
Frequency: Quarterly	Electronic publication on: www.ingineria-automobilului.ro
Total number of issues: 16	Type: Open Access
(including the December 2014 issue)	

The above constitutes series nr. 3 of SIAR scientific magazine (English version).

4. Romanian Journal of Automotive Engineering
ISSN 2457 – 5275

Period of publication: from 2015	Format: online, English
Frequency: Quarterly	Electronic publication on: www.ro-jae.ro
Total number of issues: 25 (March 2021)	Type: Open Access

The above constitutes series nr. 4 of SIAR scientific magazine (English version).

Summary

Total of series:	*4*
Total years of publication:	*27 (11: 1990 – 2000; 16: 2006 – 2021)*
Publication frequency:	*Quarterly*
Total issues published:	*88 (Romanian), out of which, the last 41 were also published in English*